On the Attainable Region for Process Networks

Jeremy A. Conner and Vasilios I. Manousiouthakis
Dept. of Chemical and Biomolecular Engineering, University of California, Los Angeles, CA 90095

DOI 10.1002/aic.14257
Published online November 21, 2013 in Wiley Online Library (wileyonlinelibrary.com)

In this work the attainable region (AR) concept for process networks with outlet flow rate specifications is introduced for the first time. For process unit models to which the infinite dimensional State-space conceptual framework is applicable, it is shown that identification of AR boundary membership is equivalent to feasibility assessment of an infinite linear program (ILP). A number of important AR properties are then theoretically established, including AR convexity, and representation of the AR in a concentration state space of reduced dimension. Finite dimensional approximations of the aforementioned ILP are then employed in creating increasingly accurate approximations of the AR. A case study for the vapor-liquid equilibrium-based separation of a ternary azeotropic mixture is used to illustrate the proposed method. The quantified two- and four-Dimensional ARs indicate that acetone mole fractions above 0.79 (acetone/methanol azeotrope) are attainable for the considered outlet flow rate ratios.
AIChE J, 60: 193–212, 2014
Keywords: process synthesis, mathematical modeling, distillation

Introduction

The attainable region (AR) for reactor networks has been the topic of substantial research effort, due to its effectiveness in rigorously assessing, at the early conceptual design stage, the limitations imposed on reactor network performance by the kinetic rates of the underlying reactions, the reactor network feed composition, and the properties of the underlying reactor units. The AR concept was first defined for reactor networks by Horn[1] as the complete set of points in concentration space that can be considered as product composition vectors of some steady-state reactor networks, using only processes of reaction and mixing/splitting from a given feed point. Glasser et al.[2] and Hildebrandt et al.[3] developed geometric methods for quantifying candidate AR's using plug-flow reactor (PFR) trajectories and continuous stirred tank reactor (CSTR) loci. Since then, several mathematical frameworks for reactor network ARs were developed; recent works include determining AR for isothermal CSTR/PFR networks,[4] nonideal reactor networks,[5] reactor networks employing variable-density fluids,[6] and batch reactor networks.[7] Computational strategies for quantifying the reactor AR abound in the literature, including "outside-in" methods such as bounding hyperplanes[8] and the Shrink-Wrap method,[4,9] as well as the Infinite DimEnsionAl State-space (IDEAS) framework.[6,10–12] Due to their vast number, we refer the reader to references within the aforementioned works for more information on AR quantification strategies.

As the reactor AR concept matured, research into coupling the reactor models with separation was carried out to identify opportunities to expand the AR for maximizing the yield of desired products. In a series of papers, Mahajani and coworkers[13–16] quantified the AR for reactive distillation networks using a generalization of the aforementioned geometric AR quantification methods. Their approach employed single-feed-single-product units termed nonazeotropic single-reactant reactive condensers/reboilers,[13] azeotropic reactive rectification and reactive stripping units,[14–16] and capitalized on the residue curve map concept formulated by Doherty et. al.[17]

Rigorous mathematical development of the AR concept for separator networks is comparatively sparse in the literature. Jobson et al.[18] examined the feasible product regions for three configurations of two vapor-liquid equilibrium (VLE) flash systems: in parallel, in series, and in series with reflux. They found cases where either configuration could outperform the others in terms of attainable product purities. Nisoli et al.[19] were the first to identify the AR for general hybrid separator/reactor/reactive-separator networks. They employed a reaction-separation vector for a two-product CSTR (multi-product CSTR series/PFR) model of a reactor/separator, to construct the AR for hybrid separator/reactor/reactive-separator networks, without inlet/outlet stream flow rate specifications, by generalizing geometric methods of reactor network AR construction. In a methyl tert-butyl ether (MTBE) case study, their method was able to identify that pure MTBE cannot be attained using a reactor network or a reactive-separator network. Rather, a reactor/separator or reactive-separator/separator network was shown to be required.

In this work, we introduce the AR concept for process networks with inlet/outlet stream flow rate specifications. This is applicable to networks with a finite number of inlets and outlets, and a possibly infinite number of process units, each of which has a finite number of inlets and outlets. The proposed process network AR concept quantifies for the first time the set of all outlet stream composition vectors that can be attained by a process network with known inlet and outlet

Correspondence concerning this article should be addressed to V.I. Manousiouthakis at vasilios@ucla.edu.

flow rate ratios. To this end, we introduce the following definition of the process network AR:

Definition. *Consider a process network with S inlets and Q outlets whose total inlet molar flow rate sum and outlet molar flow rate sum are designated as* $\sum_{i=1}^{S} F_i^U$ *and* $\sum_{i=1}^{Q} F_i^Y$*, respectively. Let the mole fraction vector* x_i^U *and the molar flow rate ratio* $\{\alpha_i^U\}_{i=1}^{S} \triangleq \left\{F_i^U / \sum_{i=1}^{S} F_i^U\right\}_{i=1}^{S}$ *of the ith inlet stream,* $i=1,S$*, be known. Let also the molar flow rate ratio* $\{\alpha_i^Y\}_{i=1}^{Q} \triangleq \left\{F_i^Y / \sum_{i=1}^{Q} F_i^Y\right\}_{i=1}^{Q}$ *of the ith outlet stream,* $i=1,Q$*, be known. Then the process network AR, denoted* $AR_{\{\alpha_i^Y\}_{i=1}^{Q},\{(\alpha_i^U,x_i^U)\}_{i=1}^{S}}$*, is defined to be the subset of the concentration space* $\Re^{Q\cdot n}$ *consisting of all* $n\cdot Q$ *dimensional vectors consisting of the n dimensional outlet mole fraction vectors of the Q products of a realizable process network.*

This definition can be equivalently expressed in terms of either mass or molar quantities; however, molar quantities are chosen to facilitate the presentation of the illustrative case study, as the associated data are given in terms of molar fractions and molar flow rates.

The rest of the article is structured as follows: first, the conceptual framework for $AR_{\{\alpha_i^Y\}_{i=1}^{Q},\{(\alpha_i^U,x_i^U)\}_{i=1}^{S}}$ will be presented in two parts. Part one will formulate the $AR_{\{\alpha_i^Y\}_{i=1}^{Q},\{(\alpha_i^U,x_i^U)\}_{i=1}^{S}}$ quantification problem using the IDEAS framework for process networks employing process units with multiple inlets and outlets. The properties of inlet/outlet flow rate independence, and convexity of the process network AR will then be established via rigorous mathematical proofs. Part two will show how the general formulation in part one translates to a separator network employing one inlet/two outlet VLE separators. We then test our method on two case studies involving separation of an azeotropic ternary mixture: one involving a separator network with one inlet stream and three outlet streams (4-D AR), and one involving a separator network with one inlet stream and two outlet streams (2-D AR). Plots demonstrating convergence of the approximated 2-D ARs and visualization of both 4-D and 2-D ARs will be provided and discussed. Lastly, conclusions will be drawn.

Conceptual Framework

IDEAS formulation for networks of process units with multiple inlets/outlets

We consider an infinite network of process units possessing a finite number of network inlets (S) and network outlets (Q), with n total species among the network streams. For simplicity of notation, we consider all process units in the network to possess the same finite number of inlets (s) and outlets (q), and consider all network streams to be at the same pressure P and to be allowed to mix. Figure 1 illustrates the IDEAS representation of the process network. This IDEAS representation breaks the process network into two components: the distribution network (DN), where all stream mixing, splitting, recycling and bypassing takes place, and the operator network (OP), consisting of all the network's process units.

The DN possesses four types of junctions: (1) those corresponding to the overall network inlet streams, and denoted with superscript U and indexed by subscript $j=1,S$; (2) those corresponding to the overall network outlet streams, and denoted with superscript Y and indexed by subscript $j=1,Q$; (3) those corresponding to the OP inlet streams, and denoted with superscript X and indexed by subscripts (i,j) $i=1,\infty$ $j=1,s$; and (4) those corresponding to the OP outlet streams, and denoted with superscript W and indexed by subscripts (i,j) $i=1,\infty$ $j=1,q$. It should be noted that Figure 1 lists all mole fraction quantities as vectors in $\Re^n$. Conservation laws are enforced at all junctions, whereas the OP includes the models describing the process units. The IDEAS formulation characterizing $AR_{\{\alpha_i^Y\}_{i=1}^{Q},\{(\alpha_i^U,x_i^U)\}_{i=1}^{S}}$ for the diagram is described by constraints (1)–(11).

Input and output flow rate ratio relations

$$F_i^U=\alpha_i^U F_{\text{tot}}^U \quad \forall i=1,S,\ \sum_{i=1}^{S}\alpha_i^U=1 \tag{1}$$

$$F_i^Y=\alpha_i^Y F_{\text{tot}}^Y \quad \forall i=1,Q,\ \sum_{i=1}^{Q}\alpha_i^Y=1 \tag{2}$$

Total mixing balances at DN junctions

$$F_j^Y=\sum_{i=1}^{\infty}\sum_{k=1}^{q}F_{j,i,k}^{YW}+\sum_{i=1}^{S}F_{j,i}^{YU} \quad \forall j=1,Q \tag{3}$$

$$F_{j,l}^X=\sum_{i=1}^{\infty}\sum_{k=1}^{q}F_{j,l,i,k}^{XW}+\sum_{i=1}^{S}F_{j,l,i}^{XU} \quad \forall j=1,\infty \quad \forall l=1,s \tag{4}$$

Total splitting balances at DN junctions

$$F_j^U=\sum_{i=1}^{\infty}\sum_{k=1}^{s}F_{i,k,j}^{XU}+\sum_{i=1}^{Q}F_{i,j}^{YU} \quad \forall j=1,S \tag{5}$$

$$F_{j,l}^W=\sum_{i=1}^{\infty}\sum_{k=1}^{s}F_{i,k,j,l}^{XW}+\sum_{i=1}^{Q}F_{i,j,l}^{YW} \quad \forall j=1,\infty \quad \forall l=1,q \tag{6}$$

Component mixing/process unit balances

$$x_j^Y F_j^Y=\sum_{i=1}^{\infty}\sum_{k=1}^{q}x_{i,k}^W F_{j,i,k}^{YW}+\sum_{i=1}^{S}x_i^U F_{j,i}^{YU} \quad \forall j=1,Q \tag{7}$$

$$f_{j,k}^X=\sum_{i=1}^{\infty}\sum_{l=1}^{q}x_{i,l}^W F_{j,k,i,l}^{XW}+\sum_{i=1}^{S}x_i^U F_{j,k,i}^{XU}, \ \forall j=1,\infty\ \forall k=1,s \tag{8}$$

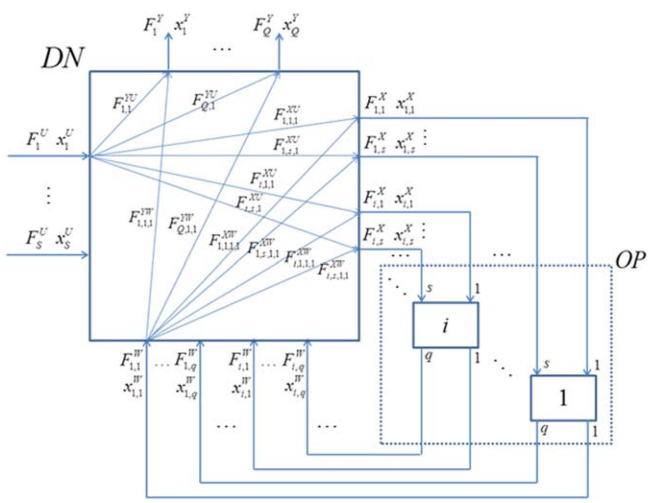

Figure 1. IDEAS diagram of a process network.

[Color figure can be viewed in the online issue, which is available at wileyonlinelibrary.com.]

IDEAS linear input species flow rate, input total flow rate, output total flow rate, and design variable relations for the jth process unit

$$0=\left[R\left(\left[x_{j,1}^{W}\right]^{\mathrm{T}},\ldots,\left[x_{j,q}^{W}\right]^{\mathrm{T}},\left[x_{j,1}^{X}\right]^{\mathrm{T}},\ldots,\left[x_{j,s}^{X}\right]^{\mathrm{T}},\left[\alpha_{j}\right]^{\mathrm{T}}\right)\right]^{\mathrm{T}}\cdot \left[\left[f_{j,1}^{X}\right]^{\mathrm{T}}\cdots\left[f_{j,s}^{X}\right]^{\mathrm{T}}F_{j,1}^{X}\cdots F_{j,s}^{X}\;F_{j,1}^{W}\cdots F_{j,q}^{W}\left[A_{j}\right]^{\mathrm{T}}\right]^{\mathrm{T}}\;\forall j=1,\infty \tag{9}$$

IDEAS composition, design parameter relations for the jth process unit

$$N\left(\left[x_{j,1}^{W}\right]^{\mathrm{T}},\ldots,\left[x_{j,q}^{W}\right]^{\mathrm{T}},\left[x_{j,1}^{X}\right]^{\mathrm{T}},\ldots,\left[x_{j,s}^{X}\right]^{\mathrm{T}},\left[\alpha_{j}\right]^{\mathrm{T}}\right)=0\;\forall j=1,\infty \tag{10}$$

The variables in the above equations must also satisfy the following positivity constraints

$$\left\{\begin{array}{l}F_{j}^{Y}\geq 0\quad\forall j=1,Q;\quad F_{j}^{U}\geq 0\quad\forall j=1,S;\\ F_{i,j}^{X}\geq 0\quad\forall i=1,\infty\quad\forall j=1,s;\quad F_{i,j}^{W}\geq 0\quad\forall i=1,\infty\quad\forall j=1,q;\\ F_{i,j}^{YU}\geq 0\quad\forall i=1,Q\quad\forall j=1,S;\quad F_{i,k,j}^{XU}\geq 0\quad\forall i=1,\infty\quad\forall k=1,s\quad\forall j=1,S\\ F_{j,i,k}^{YW}\geq 0\quad\forall j=1,Q\quad\forall i=1,\infty\quad\forall k=1,q\\ F_{j,l,i,k}^{XW}\geq 0\quad\forall j=1,\infty\quad\forall l=1,s\quad\forall i=1,\infty\quad\forall k=1,q\\ f_{j,k}^{X}\geq 0\quad\forall j=1,\infty\quad\forall k=1,s\end{array}\right\} \tag{11}$$

For a given j from 1 to ∞, Eqs. 9 and 10 capture the behavior of the jth process unit. As j varies from 1 to ∞, a subvector of the vector $\left[\left[x_{j,1}^{W}\right]^{\mathrm{T}},\ldots,\left[x_{j,q}^{W}\right]^{\mathrm{T}},\left[x_{j,1}^{X}\right]^{\mathrm{T}},\ldots,\left[x_{j,s}^{X}\right]^{\mathrm{T}},\left[\alpha_{j}\right]^{\mathrm{T}}\right]^{\mathrm{T}}$ assumes all its possible realizable values. The structure of Eq. 10 is such that, for any given j, knowledge of the aforementioned subvector guarantees knowledge of the whole vector $\left[\left[x_{j,1}^{W}\right]^{\mathrm{T}},\ldots,\left[x_{j,q}^{W}\right]^{\mathrm{T}},\left[x_{j,1}^{X}\right]^{\mathrm{T}},\ldots,\left[x_{j,s}^{X}\right]^{\mathrm{T}},\left[\alpha_{j}\right]^{\mathrm{T}}\right]^{\mathrm{T}}$. In addition, the structure of $R(\cdot)$ in 9 is such that knowledge of $\left[\left[x_{j,1}^{W}\right]^{\mathrm{T}},\ldots,\left[x_{j,q}^{W}\right]^{\mathrm{T}},\left[x_{j,1}^{X}\right]^{\mathrm{T}},\ldots,\left[x_{j,s}^{X}\right]^{\mathrm{T}},\left[\alpha_{j}\right]^{\mathrm{T}}\right]^{\mathrm{T}}$ makes $R\left(\left[x_{j,1}^{W}\right]^{\mathrm{T}},\ldots,\left[x_{j,q}^{W}\right]^{\mathrm{T}},\left[x_{j,1}^{X}\right]^{\mathrm{T}},\ldots,\left[x_{j,s}^{X}\right]^{\mathrm{T}},\left[\alpha_{j}\right]^{\mathrm{T}}\right)$ a linear operator.

It is easy to show using constraints 1, 2, along with the total concentration balance on the process network, that an equivalent AR can be defined as a subset of $\Re^{(n-1)^2}$, with corresponding flow rate ratios and concentration vectors and flow rates $\left\{a_{i}^{Y}\right\}_{i=1}^{Q-1},\left\{\left(\alpha_{i}^{U},x_{i}^{U}\right)\right\}_{i=1}^{S-1}$. This dimensional reduction significantly reduces the computational burden on quantification of the separation AR. Furthermore, as Theorem 1 demonstrates, the separation AR is convex for fixed network inlet mole fractions and fixed network inlet/outlet flow rate ratios. Therefore, techniques to quantify the AR can be employed focusing on quantification of the region's vertices, allowing for compact representation of the shape of the $AR_{\left\{\alpha_{i}^{Y}\right\}_{i=1}^{Q},\left\{\left(\alpha_{i}^{U},x_{i}^{U}\right)\right\}_{i=1}^{S}}$.

Theorem 1. *Let the units employed in a process network satisfy the IDEAS properties* 9, 10 *listed above. Then for the above process network, (a) the* $AR_{\left\{\alpha_{i}^{Y}\right\}_{i=1}^{Q},\left\{\left(\alpha_{i}^{U},x_{i}^{U}\right)\right\}_{i=1}^{S}}$ *does not depend on either* $F_{\mathrm{tot}}^{U}=\sum_{i=1}^{S}F_{i}^{U}$ *or* $F_{\mathrm{tot}}^{Y}=\sum_{i=1}^{Q}F_{i}^{Y}$, *and (b) the* $AR_{\left\{\alpha_{i}^{Y}\right\}_{i=1}^{Q},\left\{\left(\alpha_{i}^{U},x_{i}^{U}\right)\right\}_{i=1}^{S}}$ *is a convex set.*

Proof.

a. Let $\left[\left[\overline{x}_{1}^{Y}\right]^{\mathrm{T}}\cdots\left[\overline{x}_{Q}^{Y}\right]^{\mathrm{T}}\right]^{\mathrm{T}}\in AR_{\left\{\alpha_{i}^{Y}\right\}_{i=1}^{Q},\left\{\left(\alpha_{i}^{U},x_{i}^{U}\right)\right\}_{i=1}^{S}}$. Then there exists a physically realizable process network with input and output flow rate ratios $\alpha_{i}^{U}\;\forall i=1,S$, $\alpha_{i}^{Y}\;\forall i=1,Q$, design parameters $\alpha_{j}\;\forall j=1,\infty$, mole fractions $\overline{x}_{i}^{Y}\;\forall i=1,Q$; $x_{i,k}^{W}\;\forall i=1,\infty\;\forall k=1,q$; $x_{i}^{U}\;\forall i=1,S$, molar flow rates $\overline{F}_{\mathrm{tot}}^{U}$, $\overline{F}_{\mathrm{tot}}^{Y}$; $\overline{F}_{j}^{U}\;\forall j=1,S$; $\overline{F}_{j}^{Y}\;\forall j=1,Q$; $\overline{F}_{j,i,k}^{YW}\;\forall j=1,\;Q\;\forall i=1,\infty\;\forall k=1,q$, $\overline{F}_{j,i}^{YU}\;\forall j=1,Q\;\forall i=1,S$, $\overline{F}_{j,l}^{X}\;\forall j=1,\infty\;\forall l=1,s$, $\overline{F}_{j,l,i,k}^{XW}\;\forall j=1,\infty\;\forall l=1,s\;\forall i=1,\infty\;\forall k=1,q$, $\overline{F}_{j,l,i}^{XU}\;\forall j=1,\infty\;\forall l=1,\;s\;\forall i=1,S$, $\overline{F}_{j,l}^{W}\;\forall j=1,\infty\;\forall l=1,q$, component molar flow rates $\overline{f}_{j,k}^{X}\;\forall j=1,\infty\;\forall k=1,s$, and design variables $\overline{A}_{j}\;\forall j=1,\infty$ satisfying (1)–(11) Now consider a new process network with input and output flow rate ratios $\alpha_{i}^{U}\;\forall i=1,S$, $\alpha_{i}^{Y}\;\forall i=1,Q$, design parameters $\alpha_{j}\;\forall j=1,\infty$, mole fractions $\overline{x}_{i}^{Y}\;\forall i=1,Q$; $x_{i,k}^{W}\;\forall i=1,\infty\;\forall k=1,q$; $x_{i}^{U}\;\forall i=1,S$, molar flow rates $\lambda\overline{F}_{\mathrm{tot}}^{U}$, $\lambda\overline{F}_{\mathrm{tot}}^{Y}$; $\lambda\overline{F}_{j}^{U}\;\forall j=1,S$; $\lambda\overline{F}_{j}^{Y}\;\forall j=1,Q$; $\lambda\overline{F}_{j,i,k}^{YW}\;\forall j=1,\;Q\;\forall i=1,\infty\;\forall k=1,q$, $\lambda\overline{F}_{j,i}^{YU}\;\forall j=1,Q\;\forall i=1,S$, $\lambda\overline{F}_{j,l}^{X}\;\forall j=1,\;\infty\;\forall l=1,s$, $\lambda\overline{F}_{j,l,i,k}^{XW}\;\forall j=1,\infty\;\forall l=1,s\;\forall i=1,\infty\;\forall k=1,q$, $\lambda\overline{F}_{j,l,i}^{XU}\;\forall j=1,\infty\;\forall l=1,s\;\forall i=1,S$, $\lambda\overline{F}_{j,l}^{W}\;\forall j=1,\infty\;\forall l=1,q$, component molar flow rates $\lambda\overline{f}_{j,k}^{X}\;\forall j=1,\infty\;\forall k=1,s$, and design variables $\lambda\overline{A}_{j}\;\forall j=1,\infty$, where $\lambda>0$. Given the linearity of the operator R in 9, and the fact that 10 remains unchanged, it then holds that this new process network is also physically realizable, as (1)–(11) are satisfied. Thus, $\left[\left[\overline{x}_{1}^{Y}\right]^{\mathrm{T}}\cdots\left[\overline{x}_{Q}^{Y}\right]^{\mathrm{T}}\right]^{\mathrm{T}}\in AR_{\left\{\alpha_{i}^{Y}\right\}_{i=1}^{Q},\left\{\left(\alpha_{i}^{U},x_{i}^{U}\right)\right\}_{i=1}^{S}}$ continues to be true, even though $\overline{F}_{\mathrm{tot}}^{U}$ and $\overline{F}_{\mathrm{tot}}^{Y}$ have been changed to $\lambda\overline{F}_{\mathrm{tot}}^{U}$ and $\lambda\overline{F}_{\mathrm{tot}}^{Y}$. O.E.Δ.

Table 1. Wilson Coefficients (Molar Energy Differences) for Case Studies

Wilson coefficients $\left(\frac{\text{cal}}{\text{mol}}\right)$	A_{11}	A_{12}	A_{13}	A_{21}	A_{22}	A_{23}	A_{32}	A_{31}	A_{33}
W/M/A	0	469.55	1448.01	107.33	0	583.11	−161.88	291.27	0

b. We proceed by contradiction. Assume that there exist two physically realizable process networks whose composite $n\cdot Q$ dimensional exit mole fraction vectors $\left[\left[\bar{x}_1^Y\right]^T\cdots\left[\bar{x}_Q^Y\right]^T\right]^T$, $\left[\left[\hat{x}_1^Y\right]^T\cdots\left[\hat{x}_Q^Y\right]^T\right]^T$ are such that $\left[\left[\bar{x}_1^Y\right]^T\cdots\left[\bar{x}_Q^Y\right]^T\right]^T \in AR_{\{\alpha_i^Y\}_{i=1}^Q,\{(\alpha_i^U,x_i^U)\}_{i=1}^S}$ and $\left[\left[\hat{x}_1^Y\right]^T\cdots\left[\hat{x}_Q^Y\right]^T\right]^T \in AR_{\{\alpha_i^Y\}_{i=1}^Q,\{(\alpha_i^U,x_i^U)\}_{i=1}^S}$. Also assume that $\exists\lambda\in(0,1):\left[\left[\lambda\bar{x}_1^Y+(1-\lambda)\hat{x}_1^Y\right]^T\cdots\left[\lambda\bar{x}_Q^Y+(1-\lambda)\hat{x}_Q^Y\right]^T\right]^T \notin AR_{\{\alpha_i^Y\}_{i=1}^Q,\{(\alpha_i^U,x_i^U)\}_{i=1}^S}$. We will show that this leads to impossibility.

The physical realizability of the two aforementioned networks (denoted as bar and hat), combined with the lack of dependence of $AR_{\{\alpha_i^Y\}_{i=1}^Q,\{(\alpha_i^U,x_i^U)\}_{i=1}^S}$ on the total inlet and outlet network flow rate, implies that there exist input and output flow rate ratios $\alpha_i^U\left(\alpha_i^U\right)$ $\forall i=1,S$, $\alpha_i^Y\left(\alpha_i^Y\right)$ $\forall i=1,Q$, design parameters $\alpha_j\left(\alpha_j\right)$ $\forall j=1,\infty$, mole fractions $\bar{x}_i^Y\left(\hat{x}_i^Y\right)$ $\forall i=1,Q$; $x_{i,k}^W\left(x_{i,k}^W\right)$ $\forall i=1,\infty$ $\forall k=1,q$; $x_i^U\left(x_i^U\right)$ $\forall i=1,S$, molar flow rates $\bar{F}_{\text{tot}}^U=F_{\text{tot}}^U\left(\hat{F}_{\text{tot}}^U=F_{\text{tot}}^U\right)$, $\bar{F}_{tot}^Y=F_{tot}^Y\left(\hat{F}_{tot}^Y=F_{tot}^Y\right)$; $\bar{F}_j^U=F_j^U\left(\hat{F}_j^U=F_j^U\right)$ $\forall j=1,S$; $\bar{F}_j^Y=F_j^Y\left(\hat{F}_j^Y=F_j^Y\right)$ $\forall j=1,Q$; $\bar{F}_{j,i,k}^{YW}\left(\hat{F}_{j,i,k}^{YW}\right)$ $\forall j=1,Q$ $\forall i=1,\infty$ $\forall k=1,q$, $\bar{F}_{j,i}^{YU}\left(\hat{F}_{j,i}^{YU}\right)$ $\forall j=1,Q$ $\forall i=1,S$, $\bar{F}_{j,l}^X\left(\hat{F}_{j,l}^X\right)$ $\forall j=1,\infty$ $\forall l=1,s$, $\bar{F}_{j,l,i,k}^{XW}\left(\hat{F}_{j,l,i,k}^{XW}\right)$ $\forall j=1,\infty$ $\forall l=1,s$ $\forall i=1,\infty$ $\forall k=1,q$, $\bar{F}_{j,l,i}^{XU}\left(\hat{F}_{j,l,i}^{XU}\right)$ $\forall j=1,\infty$ $\forall l=1,s$ $\forall i=1,S$, $\bar{F}_{j,l}^W\left(\hat{F}_{j,l}^W\right)$ $\forall j=1,\infty$ $\forall l=1,q$, component molar flow rates $\bar{f}_{j,k}^X\left(\hat{f}_{j,k}^X\right)$ $\forall j=1,\infty$ $\forall k=1,s$, and design variables $\bar{A}_j\left(\hat{A}_j\right)$ $\forall j=1,\infty$ that satisfy the appropriate bar (hat) forms of (1)–(11). As shown in part (a) above, this implies that the following networks are also physically realizable $\forall\lambda\in[0,1]$: input and output flow rate ratios $\alpha_i^U\left(\alpha_i^U\right)$ $\forall i=1,S$, $\alpha_i^Y\left(\alpha_i^Y\right)$ $\forall i=1,Q$, design parameters $\alpha_j\left(\alpha_j\right)$ $\forall j=1,\infty$, mole fractions $\bar{x}_i^Y\left(\hat{x}_i^Y\right)$ $\forall i=1,Q$; $x_{i,k}^W\left(x_{i,k}^W\right)$ $\forall i=1,\infty$ $\forall k=1,q$; $x_i^U\left(x_i^U\right)$ $\forall i=1,S$, molar flow rates $\lambda F_{tot}^U\left((1-\lambda)F_{tot}^U\right)$, $\lambda F_{tot}^Y\left((1-\lambda)F_{tot}^Y\right)$; $\lambda F_j^U\left((1-\lambda)F_j^U\right)$ $\forall j=1,S$; $\lambda F_j^Y\left((1-\lambda)F_j^Y\right)$ $\forall j=1,Q$; $\lambda\bar{F}_{j,i,k}^{YW}\left((1-\lambda)\hat{F}_{j,i,k}^{YW}\right)$ $\forall j=1,Q$ $\forall i=1,\infty$ $\forall k=1,q$, $\lambda\bar{F}_{j,i}^{YU}\left((1-\lambda)\hat{F}_{j,i}^{YU}\right)$ $\forall j=1,Q$ $\forall i=1,S$, $\lambda\bar{F}_{j,l}^X\left((1-\lambda)\hat{F}_{j,l}^X\right)$ $\forall j=1,\infty$ $\forall l=1,s$, $\lambda\bar{F}_{j,l,i,k}^{XW}\left((1-\lambda)\hat{F}_{j,l,i,k}^{XW}\right)$ $\forall j=1,\infty$ $\forall l=1,s$ $\forall i=1,\infty$ $\forall k=1,q$, $\lambda\bar{F}_{j,l,i}^{XU}\left((1-\lambda)\hat{F}_{j,l,i}^{XU}\right)$ $\forall j=1,\infty$ $\forall l=1,s$ $\forall i=1,S$, $\lambda\bar{F}_{j,l}^W\left((1-\lambda)\hat{F}_{j,l}^W\right)$ $\forall j=1,\infty$ $\forall l=1,q$, component molar flow rates $\lambda\bar{f}_{j,k}^X\left((1-\lambda)\hat{f}_{j,k}^X\right)$ $\forall j=1,\infty$ $\forall k=1,s$, and design variables $\lambda\bar{A}_j\left((1-\lambda)\hat{A}_j\right)$ $\forall j=1,\infty$. But then, the following network is also physically realizable:

Input and output flow rate ratios α_i^U $\forall i=1,S$, α_i^Y $\forall i=1,Q$, design parameters α_j $\forall j=1,\infty$, mole fractions $\lambda\bar{x}_i^Y+(1-\lambda)\hat{x}_i^Y$ $\forall i=1,Q$; $x_{i,k}^W$ $\forall i=1,\infty$ $\forall k=1,q$; x_i^U $\forall i=1,S$, molar flow rates F_{tot}^U, F_{tot}^Y;F_j^U $\forall j=1,S$;F_j^Y $\forall j=1,Q$;$\lambda\bar{F}_{j,i,k}^{YW}+(1-\lambda)\hat{F}_{j,i,k}^{YW}$ $\forall j=1,Q$ $\forall i=1,\infty$ $\forall k=1,q$, $\lambda\bar{F}_{j,i}^{YU}+(1-\lambda)\hat{F}_{j,i}^{YU}$ $\forall j=1,Q$ $\forall i=1,S$, $\lambda\bar{F}_{j,l}^X+(1-\lambda)\hat{F}_{j,l}^X$ $\forall j=1,\infty$ $\forall l=1,s$, $\lambda\bar{F}_{j,l,i,k}^{XW}+(1-\lambda)\hat{F}_{j,l,i,k}^{XW}$ $\forall j=1,\infty$ $\forall l=1,s$ $\forall i=1,\infty$ $\forall k=1,q$, $\lambda\bar{F}_{j,l,i}^{XU}+(1-\lambda)\hat{F}_{j,l,i}^{XU}$ $\forall j=1,\infty$ $\forall l=1,s$ $\forall i=1,S$, $\lambda\bar{F}_{j,l}^W+(1-\lambda)\hat{F}_{j,l}^W$ $\forall j=1,\infty$ $\forall l=1,q$, component molar flow rates $\lambda\bar{f}_{j,k}^X+(1-\lambda)\hat{f}_{j,k}^X$ $\forall j=1,\infty$ $\forall k=1,s$, and design variables $\lambda\bar{A}_j+(1-\lambda)\hat{A}_j$ $\forall j=1,\infty$. In turn, this implies $\forall\lambda\in[0,1]:\left[\left[\lambda\bar{x}_1^Y+(1-\lambda)\hat{x}_1^Y\right]^T\cdots\left[\lambda\bar{x}_Q^Y+(1-\lambda)\hat{x}_Q^Y\right]^T\right]^T \in AR_{\{\alpha_i^Y\}_{i=1}^Q,\{(\alpha_i^U,x_i^U)\}_{i=1}^S}$. This is a contradiction. Thus $AR_{\{\alpha_i^Y\}_{i=1}^Q,\{(\alpha_i^U,x_i^U)\}_{i=1}^S}$ is a convex set. O.E.Δ.

IDEAS formulation for networks of VLE separators

The advantage of IDEAS is that it overcomes the inherently nonlinear nature of process network synthesis and optimization problems, not via some kind of Taylor series approximate linearization, but rather by exploiting the decomposition and linearity properties that the process variables naturally obey. To better demonstrate the IDEAS process network AR quantification problem, and in preparation for the case study presented later, we demonstrate how constraints (1)–(11) can be used to capture the behavior of a separator network separating a n species mixture, and employing VLE separators, each with one input ($s=1$) and two outputs ($q=2$). The considered VLE separator model will employ the Gamma-Phi VLE formulation.[20] Equations 1 and 2 remain unaltered, Eqs. 3–8 and 11 are simply specialized to $s=1$, $q=2$ and Eqs. 9 and 10 become Eqs. 12 and 13 below.

Table 2. Wilson Coefficients (Pure Species Molar Volumes) for Case Studies

Wilson coefficients $\left(\frac{\text{cm}^3}{\text{mol}}\right)$	V_1	V_2	V_3
Water/methanol/acetone	17.88	40.76	74.47

Table 3. Antoine Coefficients for Case Studies

Antoine coefficients T (K), P (bar)	Water/methanol/acetone		
	$i=1$	$i=2$	$i=3$
A_i	65.93	59.84	71.30
B_i	−7228	−6283	−5952
C_i	0	0	0
D_i	−7.177	−6.379	−8.531
E_i	4.031e-6	4.617e-6	7.824e-6
F_i	2	2	2

Table 4. Separator AR Facet-Defining Vertices for (1/16, 1/16) Discretization in $\left(x^W_{i,1,1}, x^W_{i,1,2}\right)$, $\left(x^Y_{1,1}, x^Y_{1,2}, x^Y_{2,1}, x^Y_{2,2}\right)$

#	$x^Y_{1,1}$	$x^Y_{1,2}$	$x^Y_{2,1}$	$x^Y_{2,2}$
1	0.0625	0.1875	0.125	0.6875
2	0.0625	0.1875	0.25	0.6875
3	0.0625	0.1875	0.625	0.1875
4	0.0625	0.1875	0.75	0.125
5	0.0625	0.1875	0.75	0.1875
6	0.0625	0.5625	0.625	0.3125
7	0.0625	0.625	0.75	0.1875
8	0.0625	0.6875	0.125	0.1875
9	0.0625	0.6875	0.625	0.1875
10	0.0625	0.6875	0.75	0.125
11	0.125	0.1875	0.0625	0.6875
12	0.125	0.6875	0.0625	0.1875
13	0.25	0.6875	0.0625	0.1875
14	0.25	0.6875	0.4375	0.1875
15	0.3125	0.625	0.5	0.1875
16	0.4375	0.1875	0.25	0.6875
17	0.5	0.1875	0.3125	0.625
18	0.625	0.1875	0.0625	0.1875
19	0.625	0.1875	0.0625	0.6875
20	0.625	0.3125	0.0625	0.5625
21	0.75	0.125	0.0625	0.1875
22	0.75	0.125	0.0625	0.6875
23	0.75	0.1875	0.0625	0.1875
24	0.75	0.1875	0.0625	0.625

$$\begin{aligned}0=&\left[R\left(\left[x^W_{j,1}\right]^{\mathrm{T}},\left[x^W_{j,2}\right]^{\mathrm{T}},\left[x^X_{j,1}\right]^{\mathrm{T}},\left[\alpha_j\right]^{\mathrm{T}}\right)\right]^{\mathrm{T}}\\&\cdot\left[f^X_{j,1,1}\cdots f^X_{j,1,n}\ F^X_{j,1}\ F^W_{j,1}\ F^W_{j,2}\right]^{\mathrm{T}}\\\triangleq&\begin{bmatrix}1&0\cdots&0&0&-x^W_{j,1,1}&-x^W_{j,2,1}\\0\vdots&1\ddots&0\vdots&0&\vdots&\vdots\\0&0\cdots&1&0&-x^W_{j,1,n}&-x^W_{j,2,n}\\1&1\cdots&1&-1&0&0\\0&0\cdots&0&1&-1&-1\end{bmatrix}\\&\cdot\left[f^X_{j,1,1}\cdots f^X_{j,1,n}\ F^X_{j,1}\ F^W_{j,1}\ F^W_{j,2}\right]^{\mathrm{T}}\ \forall j=1,\infty\end{aligned}\tag{12}$$

$$\begin{aligned}N:&\left[\left[x^W_{j,1}\right]^{\mathrm{T}},\left[x^W_{j,2}\right]^{\mathrm{T}},\left[x^X_{j,1}\right]^{\mathrm{T}},\left[\alpha_j\right]^{\mathrm{T}}\right]^{\mathrm{T}}\\&\rightarrow N\left(\left[x^W_{j,1}\right]^{\mathrm{T}},\left[x^W_{j,2}\right]^{\mathrm{T}},\left[x^X_{j,1}\right]^{\mathrm{T}},\left[\alpha_j\right]^{\mathrm{T}}\right)\\\triangleq&\begin{bmatrix}x^W_{j,2,1}\phi_1\left(\left\{x^W_{j,2,l}\right\}^n_{l=1},T_j,P\right)P-x^W_{j,1,1}\gamma_1\left(\left\{x^W_{j,1,l}\right\}^n_{l=1},T_j\right)P^{sat}_1(T_j)\\\vdots\\x^W_{j,2,n}\phi_n\left(\left\{x^W_{j,2,l}\right\}^n_{l=1},T_j,P\right)P-x^W_{j,1,n}\gamma_n\left(\left\{x^W_{j,1,l}\right\}^n_{l=1},T_j\right)P^{sat}_n(T_j)\\\sum_{k=1}^{n}x^W_{j,1,k}-1\\\sum_{k=1}^{n}x^W_{j,2,k}-1\end{bmatrix}=0\\&\forall j=1,\infty\end{aligned}\tag{13}$$

where

$$\left[\alpha_j\right]^{\mathrm{T}}=\left[P\quad T_j\right]\ \forall j=1,\infty\tag{14}$$

with subvector $\left[P\quad T_j\quad x^W_{j,1,1}\quad\cdots\quad x^W_{j,1,n-2}\right]\ \forall j=1,\infty$.

A variety of thermodynamic models can be employed in quantifying the functions $\phi_k\left(\left\{x^W_{j,2,l}\right\}^n_{l=1},T_j,P\right),\gamma_k\left(\left\{x^W_{j,1,l}\right\}^n_{l=1},T_j\right),P^{sat}_k(T_j)\quad\forall j=1,\infty\ \forall k=1,n$. In this demonstration, ideal gas behavior is assumed; the Wilson equations are used to model the nonideal liquid-phase activity coefficients $\gamma_k\left(\left\{x^W_{i,1,l}\right\}^n_{l=1},T_i\right)\ \forall i=1,\infty\ \forall k=1,n$; and the extended Antoine equation is used to model the species vapor pressures $P^{sat}_k(T)\ \forall k=1,n$. The relevant equations are

$$\phi_k\left(\left\{x^W_{j,2,l}\right\}^n_{l=1},T_j,P\right)=1\ \forall j=1,\infty\ \forall k=1,n\tag{15}$$

$$\begin{aligned}\ln\left(\gamma_k\left(\left\{x^W_{j,1,l}\right\}^n_{l=1},T_j\right)\right)=&1-\ln\left(\sum_{l=1}^{n}x^W_{j,1,l}\Lambda_{k,l}(T_j)\right)\\&-\sum_{l=1}^{n}\left(\frac{x^W_{j,1,l}\Lambda_{l,k}(T_j)}{\sum_{i=1}^{n}x^W_{j,1,i}\Lambda_{l,i}(T_j)}\right)\ \forall j=1,\infty\ \forall k=1,n\end{aligned}\tag{16}$$

$$\Lambda_{k,i}(T_j)=\frac{V^V_i}{V^V_k}\exp\left(\frac{-A_{k,i}}{RT_j}\right)\ \forall j=1,\infty\ \forall k=1,n;\ \forall i=1,n\tag{17}$$

$$\begin{aligned}\ln\left(P^{\mathrm{sat}}_k(T_j)\right)=&A_k+\frac{B_k}{T_j+C_k}+D_k\cdot\ln(T_j)+E_k\\&\cdot T_j^{F_k}\ \forall i=1,\infty\ \forall k=1,n\end{aligned}\tag{18}$$

Case Studies

We consider the isobaric separation of a water(1)/methanol(2)/acetone(3) mixture at $P = 1$ bar employing VLE separator units with one inlet ($s = 1$) and two outlets ($q = 2$). At these conditions, the binary mixture methanol/acetone exhibits a minimum boiling azeotrope at 0.2093/0.7907 mole fractions of methanol/acetone respectively. The thermodynamic behavior of both mixtures is captured by the Gamma-Phi VLE model described by Eqs. 15–18. The vapor phase is considered to be an ideal gas, whereas the liquid-phase activity coefficients are quantified by the Wilson Eqs. 16 and 17, and the vapor pressure of the various species is quantified by the Antoine Eq. 18. Species Wilson and Antoine coefficients for the mixture are listed in Tables 1–3. As an illustration of the versatility of the process network AR framework, we will pursue two examples: one involving a separator network with one inlet stream ($S = 1$) and three outlet streams ($Q = 3$) (4-D AR), and one involving a separator network with one inlet stream ($S = 1$) and two outlet streams ($Q = 2$) (2-D AR).

EXAMPLE 1. *We seek to identify the process network AR for a separation network with one inlet stream ($S = 1$) and three outlet streams ($Q = 3$) in which the network inlet-stream has a molar flow rate of 3 mol/s and mole fractions of 0.3, 0.35, and 0.35 for species 1, 2, and 3, respectively; that is,* $F^U_1=3\,\frac{\mathrm{mol}}{\mathrm{s}},x^U_1=\left[x^U_{1,1}\ x^U_{1,2}\ x^U_{1,3}\right]^T=[0.3\ 0.35\ 0.35]^T$. *We desire to separate this mixture into three outlet streams, each with molar flow rate of 1 mol/s,* $\left(F^Y_1=F^Y_2=F^Y_3=1\,\frac{\mathrm{mol}}{\mathrm{s}}\Rightarrow\alpha^Y_1=\alpha^Y_2=\alpha^Y_3=\frac{1}{3}\right)$, *and mole fractions* $\left[x^Y_{1,1}\ x^Y_{1,2}\ x^Y_{1,3}\right]^T,\left[x^Y_{2,1}\ x^Y_{2,2}\ x^Y_{2,3}\right]^T,\left[x^Y_{3,1}\ x^Y_{3,2}\ x^Y_{3,3}\right]^T$ *to be determined.*

Using the fact that all mole fractions must be in $[0, 1]$, the summation property of mole fractions and the total balances on species 1 and 2, we can ease the computational burden of quantifying $AR_{\left\{\alpha_i^Y\right\}_{i=1}^{Q},\left\{\left(\alpha_i^U,x_i^U\right)\right\}_{i=1}^{S}}$ by reducing its dimensionality from nine to four, and creating a set of conditions for identifying the initial superset containing it

$$\left\{\begin{array}{l} 0 \le x_{1,1}^Y \le 1, 0 \le x_{1,2}^Y \le 1, 0 \le x_{1,3}^Y \le 1 \\ 0 \le x_{2,1}^Y \le 1, 0 \le x_{2,2}^Y \le 1, 0 \le x_{2,3}^Y \le 1 \\ 0 \le x_{3,1}^Y \le 1, 0 \le x_{3,2}^Y \le 1, 0 \le x_{3,3}^Y \le 1 \\ x_{1,1}^Y + x_{1,2}^Y + x_{1,3}^Y = 1 \\ x_{2,1}^Y + x_{2,2}^Y + x_{2,3}^Y = 1 \\ x_{3,1}^Y + x_{3,2}^Y + x_{3,3}^Y = 1 \\ F_1^U x_{1,1}^U = F_1^Y x_{1,1}^Y + F_2^Y x_{2,1}^Y + F_3^Y x_{3,1}^Y \\ F_1^U x_{1,2}^U = F_1^Y x_{1,2}^Y + F_2^Y x_{2,2}^Y + F_3^Y x_{3,2}^Y \end{array}\right\} \Longleftrightarrow \left\{\begin{array}{l} 0 \le x_{1,1}^Y \le 1, 0 \le x_{1,2}^Y \le 1, 0 \le x_{1,3}^Y \le 1 \\ 0 \le x_{2,1}^Y \le 1, 0 \le x_{2,2}^Y \le 1, 0 \le x_{2,3}^Y \le 1 \\ 0 \le x_{3,1}^Y \le 1, 0 \le x_{3,2}^Y \le 1, 0 \le x_{3,3}^Y \le 1 \\ x_{1,3}^Y = 1 - x_{1,1}^Y - x_{1,2}^Y \\ x_{2,3}^Y = 1 - x_{2,1}^Y - x_{2,2}^Y \\ x_{3,3}^Y = 1 - x_{3,1}^Y - x_{3,2}^Y \\ x_{3,1}^Y = \frac{F_1^U}{F_3^Y} x_{1,1}^U - \frac{F_1^Y}{F_3^Y} x_{1,1}^Y - \frac{F_2^Y}{F_3^Y} x_{2,1}^Y \\ x_{3,2}^Y = \frac{F_1^U}{F_3^Y} x_{1,2}^U - \frac{F_1^Y}{F_3^Y} x_{1,2}^Y - \frac{F_2^Y}{F_3^Y} x_{2,2}^Y \end{array}\right\}$$

Table 5. Separator AR Facet-Defining Vertices for 1/32 Discretization in $\left(x_{i,1,1}^W, x_{i,1,2}^W\right)$, $\left(x_{1,1}^Y, x_{1,2}^Y, x_{2,1}^Y, x_{2,2}^Y\right)$

#	$x_{1,1}^Y$	$x_{1,2}^Y$	$x_{2,1}^Y$	$x_{2,2}^Y$	#	$x_{1,1}^Y$	$x_{1,2}^Y$	$x_{2,1}^Y$	$x_{2,2}^Y$
1	0.0313	0.125	0.0313	0.8125	42	0.0938	0.0938	0.75	0.21875
2	0.0313	0.125	0.0313	0.875	43	0.0938	0.84375	0.75	0.0938
3	0.0313	0.125	0.0625	0.78125	44	0.0938	0.875	0.0313	0.125
4	0.0313	0.125	0.0938	0.875	45	0.0938	0.875	0.0625	0.0938
5	0.0313	0.125	0.78125	0.0625	46	0.0938	0.875	0.125	0.0625
6	0.0313	0.125	0.8125	0.0625	47	0.0938	0.875	0.375	0.125
7	0.0313	0.125	0.8125	0.15625	48	0.0938	0.875	0.71875	0.0938
8	0.0313	0.46875	0.4375	0.53125	49	0.0938	0.875	0.75	0.0625
9	0.0313	0.78125	0.0625	0.125	50	0.125	0.0625	0.0313	0.78125
10	0.0313	0.78125	0.125	0.0625	51	0.125	0.0625	0.0313	0.90625
11	0.0313	0.78125	0.78125	0.1875	52	0.125	0.0625	0.0625	0.75
12	0.0313	0.78125	0.8125	0.15625	53	0.125	0.0625	0.0625	0.90625
13	0.0313	0.8125	0.0313	0.125	54	0.125	0.0625	0.0938	0.875
14	0.0313	0.8125	0.0625	0.0938	55	0.125	0.0625	0.6875	0.125
15	0.0313	0.84375	0.8125	0.0938	56	0.125	0.0625	0.71875	0.0938
16	0.0313	0.875	0.0313	0.125	57	0.125	0.0625	0.71875	0.25
17	0.0313	0.875	0.78125	0.0938	58	0.375	0.125	0.0938	0.875
18	0.0313	0.875	0.8125	0.0625	59	0.40625	0.0938	0.0625	0.90625
19	0.0313	0.90625	0.0625	0.0938	60	0.4375	0.0938	0.0313	0.90625
20	0.0313	0.90625	0.125	0.0625	61	0.4375	0.53125	0.0313	0.46875
21	0.0313	0.90625	0.4375	0.0938	62	0.6875	0.125	0.125	0.0625
22	0.0313	0.90625	0.78125	0.0625	63	0.71875	0.0938	0.0938	0.875
23	0.0625	0.0938	0.0313	0.8125	64	0.71875	0.0938	0.125	0.0625
24	0.0625	0.0938	0.0313	0.90625	65	0.71875	0.25	0.125	0.0625
25	0.0625	0.0938	0.0625	0.78125	66	0.75	0.0625	0.0625	0.125
26	0.0625	0.0938	0.0625	0.90625	67	0.75	0.0625	0.0625	0.90625
27	0.0625	0.0938	0.0938	0.875	68	0.75	0.0625	0.0938	0.0938
28	0.0625	0.0938	0.78125	0.0625	69	0.75	0.0625	0.0938	0.875
29	0.0625	0.0938	0.78125	0.1875	70	0.75	0.0938	0.0938	0.84375
30	0.0625	0.125	0.0313	0.78125	71	0.75	0.21875	0.0938	0.0938
31	0.0625	0.125	0.0625	0.75	72	0.78125	0.0625	0.0313	0.125
32	0.0625	0.125	0.75	0.0625	73	0.78125	0.0625	0.0313	0.90625
33	0.0625	0.75	0.0625	0.125	74	0.78125	0.0625	0.0625	0.0938
34	0.0625	0.75	0.125	0.0625	75	0.78125	0.0938	0.0313	0.875
35	0.0625	0.78125	0.0313	0.125	76	0.78125	0.1875	0.0313	0.78125
36	0.0625	0.78125	0.0625	0.0938	77	0.78125	0.1875	0.0625	0.0938
37	0.0625	0.90625	0.0625	0.0938	78	0.8125	0.0625	0.0313	0.125
38	0.0625	0.90625	0.125	0.0625	79	0.8125	0.0625	0.0313	0.875
39	0.0625	0.90625	0.40625	0.0938	80	0.8125	0.0938	0.0313	0.84375
40	0.0625	0.90625	0.75	0.0625	81	0.8125	0.15625	0.0313	0.125
41	0.0938	0.0938	0.75	0.0625	82	0.8125	0.15625	0.0313	0.78125

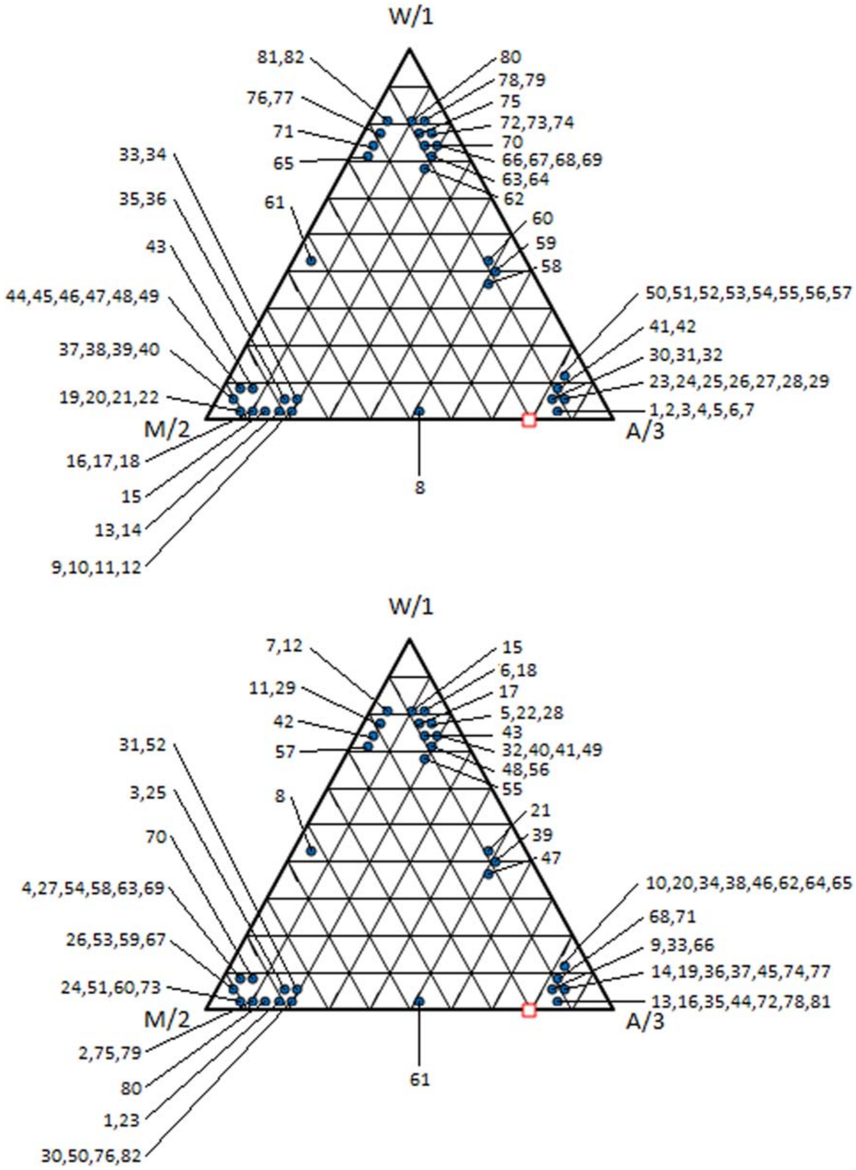

Figure 2. Ternary diagrams for network product streams 1 and 2.

[Color figure can be viewed in the online issue, which is available at wileyonlinelibrary.com.]

Substitution of $x^Y_{1,3}, x^Y_{2,3}, x^Y_{3,1}, x^Y_{3,2}, x^Y_{3,3}$ yields the following equivalent inequalities

$$\left\{\begin{array}{l} 0 \le x^Y_{1,1} \le 1, 0 \le x^Y_{1,2} \le 1, 0 \le x^Y_{2,1} \le 1, 0 \le x^Y_{2,2} \le 1 \\ 0 \le 1 - x^Y_{1,1} - x^Y_{1,2} \le 1 \\ 0 \le 1 - x^Y_{2,1} - x^Y_{2,2} \le 1 \\ \dfrac{F^U_1}{F^Y_3} x^U_{1,1} - 1 \le \dfrac{F^Y_1}{F^Y_3} x^Y_{1,1} + \dfrac{F^Y_2}{F^Y_3} x^Y_{2,1} \le \dfrac{F^U_1}{F^Y_3} x^U_{1,1} \\ \dfrac{F^U_1}{F^Y_3} x^U_{1,2} - 1 \le \dfrac{F^Y_1}{F^Y_3} x^Y_{1,2} + \dfrac{F^Y_2}{F^Y_3} x^Y_{2,2} \le \dfrac{F^U_1}{F^Y_3} x^U_{1,2} \\ \dfrac{F^U_1}{F^Y_3} \left(x^U_{1,1} + x^U_{1,2} \right) - 1 \le \dfrac{F^Y_1}{F^Y_3} \left(x^Y_{1,1} + x^Y_{1,2} \right) + \dfrac{F^Y_2}{F^Y_3} \left(x^Y_{2,1} + x^Y_{2,2} \right) \le \dfrac{F^U_1}{F^Y_3} \left(x^U_{1,1} + x^U_{1,2} \right) \end{array}\right\} \tag{19}$$

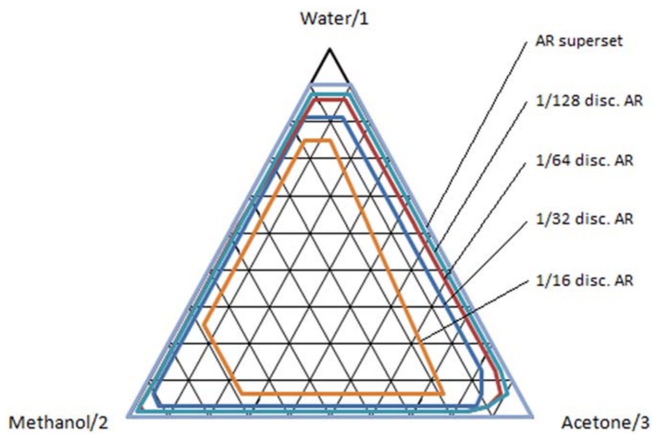

Figure 3. 2-D AR approximants and AR superset.

[Color figure can be viewed in the online issue, which is available at wileyonlinelibrary.com.]

For our known values, constraint set 19 becomes

$$\begin{Bmatrix} 0 \le x^Y_{1,1} \le 1, 0 \le x^Y_{1,2} \le 1, 0 \le x^Y_{2,1} \le 1, 0 \le x^Y_{2,2} \le 1 \\ 0 \le 1 - x^Y_{1,1} - x^Y_{1,2} \le 1 \\ 0 \le 1 - x^Y_{2,1} - x^Y_{2,2} \le 1 \\ -0.1 \le x^Y_{1,1} + x^Y_{2,1} \le 0.9 \\ 0.05 \le x^Y_{1,2} + x^Y_{2,2} \le 1.05 \\ 0.95 \le x^Y_{1,1} + x^Y_{1,2} + x^Y_{2,1} + x^Y_{2,2} \le 1.95 \end{Bmatrix} \tag{20}$$

To approximate solution of the infinite linear program (ILP) for $AR_{\{\alpha_i^Y\}_{i=1}^Q, \{(\alpha_i^U, x_i^U)\}_{i=1}^S}$ quantification, we consider only a finite number of values for the network outlet mole fractions and the VLE separator subvector parameters. From the Gibbs phase rule, by fixing the operating pressure of the entire network, we only need to select two design parameters to fully specify a VLE separator. For our case study, we choose the *i*th VLE separator outlet 1, species 1 and species 2 mole fractions $\left(x^W_{i,1,1}, x^W_{i,1,2}\right)$ as the two design parameters. Discretization levels of 1/16 and 1/32 for $\left(x^W_{i,1,1}, x^W_{i,1,2}\right)$ and for the network outlets $\left(x^Y_{1,1}, x^Y_{1,2}, x^Y_{2,1}, x^Y_{2,2}\right)$ will be employed. Calculation of the approximate $AR_{\{\alpha_i^Y\}_{i=1}^Q, \{(\alpha_i^U, x_i^U)\}_{i=1}^S}$ for each of these discretizations is pursued through solution of an LP feasibility problem formulation of IDEAS using a Fortran (MINOS v. 5.5) implementation, for all grid points in the above identified AR superset. The algorithm first generates a family of VLE separator units using the discretized subvector parameters and the thermodynamic model, then, for each combination of $x^Y_{1,1}, x^Y_{1,2}, x^Y_{2,1}, x^Y_{2,2}$, attempts to construct a feasible separator network using only the generated VLE separator units and interconnecting streams.

The facet-defining vertices of the 4-D approximate ARs for the 1/16 and 1/32 discretization levels are shown in Tables 4 and 5. Close examination of the facet point list reveals that for any combination $\left(x^Y_{1,1}, x^Y_{1,2}, x^Y_{2,1}, x^Y_{2,2}\right)$, the combination $\left(x^Y_{2,1}, x^Y_{2,2}, x^Y_{1,1}, x^Y_{1,2}\right)$ also appears. This is a manifestation of the equal network outlet flow rate ratios, which allows for interchange of network outlet concentration combinations among the outlet streams with appropriate rearrangement of the network's VLE separator units and streams. A visual representation of the aforementioned facet-defining vertices for the 1/32 discretization level is also provided in Figure 2. This graphical representation illustrates each vertex point by depicting its corresponding composition of stream 1 in one ternary diagram, and its corresponding composition of stream 2 in another ternary diagram. As many vertices share stream 1 or stream 2 compositions, the list of vertices corresponding to a particular stream composition must be shown on the diagram. For example, from Table 5, the 50th vertex has coordinates $\left(x^Y_{1,1}, x^Y_{1,2}, x^Y_{2,1}, x^Y_{2,2}\right) = (0.125, 0.0625, 0.0313, 0.78125)$. It is illustrated in Figure 2 through its stream 1 composition

Table 6. AR Vertices for 1/128 Discretization

#	$x^Y_{1,1}$	$x^Y_{1,2}$
1	0.015625	0.15625
2	0.015625	0.96875
3	0.03125	0.09375
4	0.03125	0.95313
5	0.046875	0.0625
6	0.0625	0.03125
7	0.09375	0.89063
8	0.125	0.015625
9	0.875	0.015625
10	0.875	0.10938

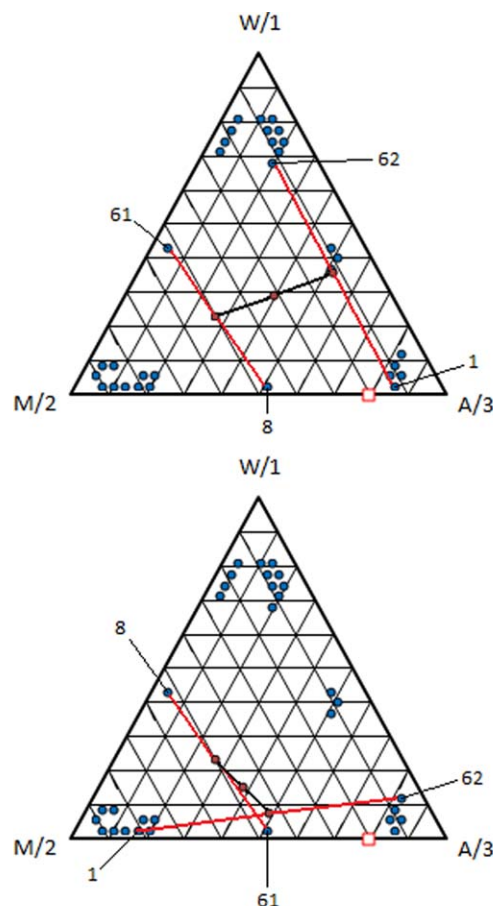

Figure 4. Graphical assessment of product feasibility.

[Color figure can be viewed in the online issue, which is available at wileyonlinelibrary.com.]

Table 7. List of Streams in the DN

Stream #	Type	Dest.	Source	Flowrate	Stream #	Type	Dest.	Source	Flowrate
1	FXU	41	Inlet 1	0.025601273	177	FXW1	115	63	0.477508051
2	FXU	74	Inlet 1	1.073101297	178	FXW1	115	97	0.632153845
3	FXU	82	Inlet 1	0.505750201	179	FXW1	115	104	1.828670108
4	FXU	99	Inlet 1	0.589710595	180	FXW1	115	114	3.570144406
5	FXU	113	Inlet 1	0.80583663	181	FXW1	116	108	3.312313154
6	FYW2	Outlet 1	2	0.290348384	182	FXW1	116	115	3.766865006
7	FYW2	Outlet 1	19	0.419084135	183	FXW1	117	86	1.453216878
8	FYW2	Outlet 1	20	0.29056748	184	FXW1	117	110	0.799170949
9	FYW1	Outlet 2	17	0.996392739	185	FXW1	117	116	2.325703317
10	FYW1	Outlet 2	34	0.001992062	186	FXW2	2	3	0.397021459
11	FYW2	Outlet 2	33	0.0016152	187	FXW2	2	20	0.38516223
12	FYW1	Outlet 3	110	0.371885657	188	FXW2	3	4	0.384044757
13	FYW1	Outlet 3	116	0.228113709	189	FXW2	3	21	0.116518064
14	FYW1	Outlet 3	117	0.400000634	190	FXW2	4	5	0.316227892
15	FXW1	3	2	0.491835285	191	FXW2	4	23	0.851300118
16	FXW1	7	54	0.188854384	192	FXW2	5	6	0.238451337
17	FXW1	8	7	0.882431694	193	FXW2	5	24	0.382759133
18	FXW1	9	8	1.203431356	194	FXW2	6	7	0.416086711
19	FXW1	10	9	2.010337308	195	FXW2	6	40	0.182505559
20	FXW1	11	10	1.482266564	196	FXW2	7	8	2.529760072
21	FXW1	13	11	0.395978404	197	FXW2	7	26	0.889407201
22	FXW1	14	12	0.662086058	198	FXW2	8	9	2.57829769
23	FXW1	14	13	0.023228666	199	FXW2	8	27	1.255730875
24	FXW1	15	13	0.810607318	200	FXW2	8	43	0.486323609
25	FXW1	16	14	0.68690578	201	FXW2	8	66	0.088275879
26	FXW1	16	15	0.028019254	202	FXW2	9	10	2.804739755
27	FXW1	18	17	0.426919956	203	FXW2	9	28	0.533142651
28	FXW1	20	19	0.610784287	204	FXW2	9	44	0.718685941
29	FXW1	21	3	0.595376663	205	FXW2	10	11	2.159597508
30	FXW1	21	20	1.019156895	206	FXW2	10	29	1.418995188
31	FXW1	22	21	0.852493006	207	FXW2	11	12	0.830953851
32	FXW1	23	4	0.78348326	208	FXW2	11	13	1.17098543
33	FXW1	24	5	0.304982584	209	FXW2	11	30	0.339333664
34	FXW1	24	23	0.015674673	210	FXW2	12	14	0.327253733
35	FXW1	26	7	1.422385327	211	FXW2	12	31	1.165786181
36	FXW1	27	8	1.557868352	212	FXW2	13	14	0.750018054
37	FXW1	27	26	0.408847636	213	FXW2	13	15	0.09538801
38	FXW1	28	9	0.671364681	214	FXW2	13	32	0.763436965
39	FXW1	28	27	0.242237841	215	FXW2	14	15	1.078862839
40	FXW1	29	10	1.301923728	216	FXW2	15	16	1.178602844
41	FXW1	29	28	0.066651258	217	FXW2	16	17	1.32197857
42	FXW1	30	11	0.186231173	218	FXW2	16	49	0.168211212
43	FXW1	31	11	1.081732395	219	FXW2	17	18	0.43041733
44	FXW1	31	29	0.175557522	220	FXW2	17	33	2.67460021
45	FXW1	32	30	0.087833143	221	FXW2	18	33	0.042097153
46	FXW1	33	15	0.786940053	222	FXW2	18	34	1.138255808
47	FXW1	33	16	1.026511968	223	FXW2	19	20	0.505852481
48	FXW1	34	17	0.218140596	224	FXW2	19	35	0.524015946
49	FXW1	34	18	1.176855585	225	FXW2	20	21	1.164422618
50	FXW1	36	20	0.000676911	226	FXW2	20	36	0.426209046
51	FXW1	37	21	0.418020675	227	FXW2	21	22	0.573994127
52	FXW1	38	23	1.063261653	228	FXW2	21	37	0.37073228
53	FXW1	39	24	0.459484545	229	FXW2	22	23	0.53190921
54	FXW1	41	54	0.016155129	230	FXW2	23	24	0.278711548
55	FXW1	43	42	0.141488721	231	FXW2	23	38	1.399950866
56	FXW1	44	27	0.468747254	232	FXW2	24	25	0.184208634
57	FXW1	45	28	0.31380861	233	FXW2	24	39	0.616089334
58	FXW1	45	29	0.084906636	234	FXW2	25	7	0.157618653
59	FXW1	46	29	0.442026221	235	FXW2	25	54	0.168504774
60	FXW1	47	29	0.126645492	236	FXW2	26	66	0.097971758
61	FXW1	47	30	0.197013146	237	FXW2	29	45	0.879556065
62	FXW1	48	31	0.826821833	238	FXW2	30	46	0.437948776
63	FXW1	48	32	1.042040513	239	FXW2	31	47	0.735318091
64	FXW1	49	32	0.1312026	240	FXW2	32	48	1.848846914
65	FXW1	50	33	2.180156604	241	FXW2	33	17	0.141585691
66	FXW1	50	34	0.254748314	242	FXW2	33	50	2.943431461
67	FXW1	51	35	0.342829151	243	FXW2	35	51	0.829741434
68	FXW1	52	36	0.248251537	244	FXW2	35	52	0.037103693
69	FXW1	53	21	0.007805616	245	FXW2	36	52	0.614354092
70	FXW1	54	73	0.132915213	246	FXW2	36	53	0.059429576
71	FXW1	55	64	1.002215997	247	FXW2	37	95	0.074938263
72	FXW1	57	44	0.209332649	248	FXW2	38	63	0.653537243
73	FXW1	58	45	0.496132292	249	FXW2	38	72	0.689689837

TABLE 7. *Continued*

Stream #	Type	Dest.	Source	Flowrate	Stream #	Type	Dest.	Source	Flowrate
74	FXW1	59	46	0.823935433	250	FXW2	39	40	0.025283155
75	FXW1	59	47	0.008870187	251	FXW2	39	73	0.775188485
76	FXW1	60	47	0.035314391	252	FXW2	40	7	0.084311382
77	FXW1	60	48	0.018033187	253	FXW2	40	74	0.310661704
78	FXW1	61	48	0.188116707	254	FXW2	41	26	0.121727088
79	FXW1	61	49	0.056430827	255	FXW2	42	43	0.364281346
80	FXW1	61	50	0.890022633	256	FXW2	42	66	2.110303334
81	FXW1	62	116	0.000807198	257	FXW2	43	67	1.754106195
82	FXW1	63	103	0.088704947	258	FXW2	44	57	0.430342973
83	FXW1	64	6	0.360140921	259	FXW2	44	77	0.190872932
84	FXW1	64	25	0.141914789	260	FXW2	45	58	0.476245912
85	FXW1	64	73	1.813920674	261	FXW2	45	68	0.500727216
86	FXW1	65	41	0.07627014	262	FXW2	46	78	0.81985798
87	FXW1	65	74	0.064304317	263	FXW2	47	59	0.62113424
88	FXW1	66	42	0.908783791	264	FXW2	47	69	0.100897021
89	FXW1	67	43	1.044989977	265	FXW2	48	60	0.028430725
90	FXW1	68	44	0.161944564	266	FXW2	48	69	0.863622867
91	FXW1	69	59	0.516864361	267	FXW2	49	61	0.093439438
92	FXW1	69	70	0.639604747	268	FXW2	50	61	1.398549177
93	FXW1	70	47	0.266187231	269	FXW2	51	71	0.531883612
94	FXW1	70	48	0.705919111	270	FXW2	51	85	0.010686642
95	FXW1	70	60	0.024916853	271	FXW2	51	93	0.852147396
96	FXW1	70	61	0.751332768	272	FXW2	51	101	0.030580512
97	FXW1	71	51	0.938385902	273	FXW2	52	62	0.034930734
98	FXW1	71	117	0.027332904	274	FXW2	52	86	1.122435479
99	FXW1	72	38	1.006537857	275	FXW2	53	79	0.091588954
100	FXW1	72	97	0.25928816	276	FXW2	54	7	0.645187921
101	FXW1	73	39	0.643866853	277	FXW2	54	99	1.254120246
102	FXW1	73	89	0.690793749	278	FXW2	55	26	0.100375158
103	FXW1	74	40	0.187184382	279	FXW2	55	42	1.42431213
104	FXW1	74	54	0.709710703	280	FXW2	55	75	0.800573408
105	FXW1	75	55	1.482378152	281	FXW2	57	77	0.501847831
106	FXW1	76	66	2.493172893	282	FXW2	58	84	0.536195135
107	FXW1	78	58	0.556081519	283	FXW2	59	78	0.305192979
108	FXW1	78	69	1.079353838	284	FXW2	61	70	1.108751216
109	FXW1	79	53	0.039964995	285	FXW2	62	87	0.053443302
110	FXW1	80	97	1.395979289	286	FXW2	63	89	1.171566566
111	FXW1	81	89	0.320004513	287	FXW2	64	41	0.087213352
112	FXW1	82	64	1.281182285	288	FXW2	64	55	1.84509859
113	FXW1	83	65	0.121206754	289	FXW2	64	82	0.78451215
114	FXW1	84	57	0.280837512	290	FXW2	65	83	0.061034803
115	FXW1	84	68	0.341140608	291	FXW2	66	76	1.014358872
116	FXW1	84	78	1.132184812	292	FXW2	66	91	0.523239177
117	FXW1	85	117	0.00191989	293	FXW2	66	109	3.015335268
118	FXW1	86	106	0.750284576	294	FXW2	67	100	0.98904611
119	FXW1	87	62	0.019319768	295	FXW2	67	105	2.0645537
120	FXW1	87	107	0.621656651	296	FXW2	68	84	0.005632511
121	FXW1	88	115	0.201083347	297	FXW2	68	92	0.674290749
122	FXW1	89	63	0.129226265	298	FXW2	69	78	0.887404603
123	FXW1	89	72	0.576136175	299	FXW2	73	54	0.948998371
124	FXW1	89	104	1.331669357	300	FXW2	73	64	2.749402135
125	FXW1	90	73	2.510830887	301	FXW2	73	90	1.043576949
126	FXW1	90	98	0.042928282	302	FXW2	73	115	2.536186725
127	FXW1	91	66	0.040967426	303	FXW2	74	65	0.080402508
128	FXW1	92	67	2.344483549	304	FXW2	75	112	1.006281643
129	FXW1	92	77	0.412559319	305	FXW2	76	109	0.640477521
130	FXW1	92	84	1.175537129	306	FXW2	77	100	1.027374203
131	FXW1	93	71	0.433835189	307	FXW2	77	105	0.077905891
132	FXW1	93	117	0.186175315	308	FXW2	78	84	1.336025619
133	FXW1	94	110	0.279849525	309	FXW2	78	92	0.173179414
134	FXW1	95	107	1.341726952	310	FXW2	79	95	1.737067529
135	FXW1	96	102	2.06538789	311	FXW2	79	117	0.477209759
136	FXW1	97	96	2.432527961	312	FXW2	80	73	1.521852702
137	FXW1	97	115	0.00434133	313	FXW2	80	98	0.961953875
138	FXW1	98	80	2.102554537	314	FXW2	81	74	0.438145492
139	FXW1	99	81	0.368630887	315	FXW2	83	112	0.003145134
140	FXW1	100	66	0.631025835	316	FXW2	84	92	1.299227462
141	FXW1	100	76	2.119291549	317	FXW2	85	101	0.015117104
142	FXW1	100	92	1.898894212	318	FXW2	86	107	1.825367769
143	FXW1	101	117	0.02659968	319	FXW2	87	102	2.346343756
144	FXW1	102	37	0.122226652	320	FXW2	87	117	0.183933748
145	FXW1	102	79	0.808054397	321	FXW2	88	104	0.983034553
146	FXW1	102	87	1.121769395	322	FXW2	89	73	1.858116839

TABLE 7. *Continued*

Stream #	Type	Dest.	Source	Flowrate	Stream #	Type	Dest.	Source	Flowrate
147	FXW1	102	107	1.266994637	323	FXW2	89	81	0.206427796
148	FXW1	103	102	0.522760182	324	FXW2	91	109	0.686308976
149	FXW1	104	88	0.592459676	325	FXW2	92	100	0.113011839
150	FXW1	104	103	0.435165606	326	FXW2	93	106	0.910335046
151	FXW1	105	75	1.688086386	327	FXW2	94	107	0.792236208
152	FXW1	105	83	0.063317083	328	FXW2	95	108	2.492081079
153	FXW1	105	91	0.204037219	329	FXW2	96	88	0.092916855
154	FXW1	105	100	2.519779444	330	FXW2	96	97	1.926679354
155	FXW1	106	85	0.006350353	331	FXW2	97	80	1.777231397
156	FXW1	106	93	0.678198154	332	FXW2	98	81	0.183091343
157	FXW1	106	117	0.137480759	333	FXW2	99	114	2.051247413
158	FXW1	107	94	0.488225049	334	FXW2	101	110	0.075813889
159	FXW1	107	116	1.826438323	335	FXW2	102	96	1.652456138
160	FXW1	108	22	0.810408087	336	FXW2	103	104	0.453357513
161	FXW1	108	87	0.290361418	337	FXW2	104	89	0.870990652
162	FXW1	108	95	2.021802148	338	FXW2	104	116	3.735997826
163	FXW1	108	111	1.730833988	339	FXW2	105	109	0.439735304
164	FXW1	109	105	2.772495876	340	FXW2	106	110	0.838590362
165	FXW1	110	52	0.754159926	341	FXW2	107	79	0.172487607
166	FXW1	110	101	0.056715953	342	FXW2	107	87	1.705679735
167	FXW1	110	117	0.970573819	343	FXW2	107	111	1.655151418
168	FXW1	112	74	1.237287353	344	FXW2	108	88	0.498741399
169	FXW1	112	82	1.002420324	345	FXW2	108	103	0.452247149
170	FXW1	112	99	1.755468668	346	FXW2	109	112	5.863701022
171	FXW1	112	109	3.854339829	347	FXW2	110	94	0.583860678
172	FXW1	113	90	1.510182236	348	FXW2	111	102	0.037009425
173	FXW1	113	112	3.320327604	349	FXW2	111	117	3.348975982
174	FXW1	114	89	1.048220886	350	FXW2	112	113	2.343939228
175	FXW1	114	98	1.280763691	351	FXW2	116	104	1.037882126
176	FXW1	114	113	3.292407242	352	FXW2	117	79	1.182111359

$\left(x^Y_{1,1}, x^Y_{1,2}\right)=(0.125, 0.0625)$, shown in the bottom right corner of the first ternary diagram and identified through the number 50, and through its stream 2 composition $\left(x^Y_{2,1}, x^Y_{2,2}\right)=(0.0313, 0.78125)$, shown in the bottom left corner of the second ternary diagram and also identified through the number 50.

Another visual representation of the 4-D approximate AR corresponding to the 1/16 discretization level is shown in Appendix A. There, 2-D projections of the aforementioned AR are shown for every composition of stream 1 corresponding to the composition grid generated by the 1/16 discretization level. These projections were generated by taking the convex hull of all points in $AR_{\{\alpha^Y_i\}^Q_{i=1},\{(\alpha^U_i,x^U_i)\}^S_{i=1}}$ corresponding to each stream 1 mole fraction combination in Table 5.

Example 2. *In this example, we seek to identify the process network AR for a separation network with one inlet stream ($S=1$) and two outlet streams ($Q=2$) in which the network inlet stream has a molar flow rate of 3 mol/s and mole fractions of 0.3, 0.35, and 0.35 for species 1, 2, and 3, respectively; that is,* $F^U_1=3\,\frac{\text{mol}}{\text{s}}, x^U_1=\left[x^U_{1,1}\ x^U_{1,2}\ x^U_{1,3}\right]^T=[0.3\ 0.35\ 0.35]^T$. *We desire to separate this mixture into two outlet streams, one with molar flow rate of 1 mol/s, and the other with molar flow rate of 2 mol/s* $\left(F^Y_1=1\,\frac{\text{mol}}{\text{s}}, F^Y_2=2\,\frac{\text{mol}}{\text{s}} \Rightarrow \alpha^Y_1=\frac{1}{3}, \alpha^Y_2=\frac{2}{3}\right)$, *and mole fractions* $\left[x^Y_{1,1}\ x^Y_{1,2}\ x^Y_{1,3}\right]^T, \left[x^Y_{2,1}\ x^Y_{2,2}\ x^Y_{2,3}\right]^T$ *to be determined.*

As in example 1, all mole fractions must be in $[0,1]$, the summation property of mole fractions must hold, and the total balances on species 1 and 2 must also hold. Then we can ease the computational burden of quantifying $AR_{\{\alpha^Y_i\}^Q_{i=1},\{(\alpha^U_i,x^U_i)\}^S_{i=1}}$ by reducing its dimensionality from six to two, and creating a set of conditions for identifying the initial superset containing it. This is identified in a similar manner as before:

$$\left\{\begin{array}{l} 0 \le x^Y_{1,1} \le 1 \\ 0 \le x^Y_{1,2} \le 1 \\ 0 \le 1-x^Y_{1,1}-x^Y_{1,2} \le 1 \\ \frac{F^U_1}{F^Y_1}x^U_{1,1} \ge x^Y_{1,1} \ge \frac{F^U_1}{F^Y_1}x^U_{1,1}-\frac{F^Y_2}{F^Y_1} \\ \frac{F^U_1}{F^Y_1}x^U_{1,2} \ge x^Y_{1,2} \ge \frac{F^U_1}{F^Y_1}x^U_{1,2}-\frac{F^Y_2}{F^Y_1} \\ \frac{F^U_1}{F^Y_1}x^U_{1,1}+\frac{F^U_1}{F^Y_1}x^U_{1,2}-\frac{F^Y_2}{F^Y_1} \le x^Y_{1,1}+x^Y_{1,2} \le \frac{F^U_1}{F^Y_1}x^U_{1,1}+\frac{F^U_1}{F^Y_1}x^U_{1,2} \end{array}\right\} \tag{21}$$

For our known values $\left(F^U_1=3,\ F^Y_1=1,\ F^Y_2=2,\ x^U_{1,1}=0.3,\ x^U_{1,2}=0.35\right)$, constraint set (21) becomes:

$$\left\{\begin{array}{l} 0 \le x^Y_{1,1} \le 1 \\ 0 \le x^Y_{1,2} \le 1 \\ 0 \le 1-x^Y_{1,1}-x^Y_{1,2} \le 1 \\ -1.1 \le x^Y_{1,1} \le 0.9 \\ -0.95 \le x^Y_{1,2} \le 1.05 \\ -0.05 \le x^Y_{1,1}+x^Y_{1,2} \le 1.95 \end{array}\right\} \tag{22}$$

Table 8. List of VLE Separators Used in the Network

T	VLE sep. #	$x^W_{i,1,1}$	$x^W_{i,1,2}$	$x^W_{i,2,1}$	$x^W_{i,2,2}$
55.49072	2	0.03125	0.15625	0.018231	0.159447
55.47973	3	0.03125	0.1875	0.017446	0.185926
55.5327	4	0.03125	0.25	0.016096	0.235561
55.67462	5	0.03125	0.3125	0.014986	0.282039
55.8985	6	0.03125	0.375	0.014071	0.326696
56.20333	7	0.03125	0.4375	0.013317	0.370757
56.59512	8	0.03125	0.5	0.012703	0.415463
57.08185	9	0.03125	0.5625	0.012216	0.462096
57.68052	10	0.03125	0.625	0.011847	0.512202
58.41611	11	0.03125	0.6875	0.011597	0.567714
58.84488	12	0.03125	0.71875	0.011519	0.598249
59.32162	13	0.03125	0.75	0.011473	0.631159
59.85332	14	0.03125	0.78125	0.011464	0.666939
60.446	15	0.03125	0.8125	0.011493	0.706136
61.11063	16	0.03125	0.84375	0.011566	0.749514
61.85822	17	0.03125	0.875	0.011689	0.797977
62.69976	18	0.03125	0.90625	0.011868	0.85259
55.90849	19	0.0625	0.09375	0.037328	0.099006
55.86252	20	0.0625	0.125	0.035665	0.12807
55.84353	21	0.0625	0.15625	0.034163	0.155635
55.85052	22	0.0625	0.1875	0.032805	0.18194
55.93448	23	0.0625	0.25	0.030455	0.231585
56.10538	24	0.0625	0.3125	0.028516	0.27849
56.35925	25	0.0625	0.375	0.026915	0.323965
57.12982	26	0.0625	0.5	0.024548	0.415657
57.66753	27	0.0625	0.5625	0.023731	0.464613
58.33316	28	0.0625	0.625	0.023148	0.517899
59.15671	29	0.0625	0.6875	0.022808	0.577779
59.64144	30	0.0625	0.71875	0.022738	0.611144
60.18214	31	0.0625	0.75	0.02274	0.647403
60.78881	32	0.0625	0.78125	0.022823	0.687217
63.10754	33	0.0625	0.875	0.023665	0.836459
64.09499	34	0.0625	0.90625	0.024201	0.900261
56.60311	35	0.125	0.0625	0.068274	0.064823
56.56713	36	0.125	0.09375	0.065523	0.094599
56.57113	37	0.125	0.15625	0.060753	0.150072
56.75303	38	0.125	0.25	0.055093	0.226133
56.9839	39	0.125	0.3125	0.052122	0.274147
57.30473	40	0.125	0.375	0.04969	0.321563
57.7235	41	0.125	0.4375	0.047743	0.36975
58.2562	42	0.125	0.5	0.046257	0.420262
58.92583	43	0.125	0.5625	0.045231	0.474969
59.76737	44	0.125	0.625	0.044697	0.536332
60.82879	45	0.125	0.6875	0.044722	0.607735
61.46244	46	0.125	0.71875	0.04498	0.648663
62.18105	47	0.125	0.75	0.045436	0.694207
62.9966	48	0.125	0.78125	0.046116	0.745391
63.92709	49	0.125	0.8125	0.047064	0.80363
64.9925	50	0.125	0.84375	0.048333	0.870719
57.24976	51	0.1875	0.0625	0.090843	0.062657
57.24576	52	0.1875	0.09375	0.087693	0.09179
57.26675	53	0.1875	0.125	0.084822	0.119744
58.29418	54	0.1875	0.375	0.069604	0.323178
58.82089	55	0.1875	0.4375	0.067581	0.37521
61.45544	57	0.1875	0.625	0.065925	0.567042
62.88066	58	0.1875	0.6875	0.067317	0.656033
63.75018	59	0.1875	0.71875	0.068546	0.709079
64.74963	60	0.1875	0.75	0.070225	0.769821
65.905	61	0.1875	0.78125	0.072457	0.840411
57.98435	62	0.25	0.125	0.102785	0.11811
58.4441	63	0.25	0.25	0.093449	0.223671
59.3546	64	0.25	0.375	0.08769	0.329141
60.03323	65	0.25	0.4375	0.086151	0.386521
60.91274	66	0.25	0.5	0.085624	0.450503
62.05711	67	0.25	0.5625	0.086318	0.525096
63.56329	68	0.25	0.625	0.088617	0.616485
65.57418	69	0.25	0.6875	0.093177	0.734776
66.83349	70	0.25	0.71875	0.096648	0.8091
58.55904	71	0.3125	0.0625	0.124084	0.060894
59.34061	72	0.3125	0.25	0.109352	0.226503
59.85332	73	0.3125	0.3125	0.106582	0.281723
60.53495	74	0.3125	0.375	0.104938	0.34041
61.43546	75	0.3125	0.4375	0.104595	0.405587
62.6288	76	0.3125	0.5	0.105868	0.481616
64.22592	77	0.3125	0.5625	0.109317	0.5753
66.39873	78	0.3125	0.625	0.115952	0.69816
59.44655	79	0.375	0.125	0.131528	0.118926
60.30708	80	0.375	0.25	0.124231	0.232456
60.9927	81	0.375	0.3125	0.122571	0.292548
61.91519	82	0.375	0.375	0.122513	0.358883
63.16051	83	0.375	0.4375	0.124512	0.436192
67.22128	84	0.375	0.5625	0.138584	0.659551
59.88131	85	0.4375	0.0625	0.14855	0.061927
60.03123	86	0.4375	0.09375	0.146032	0.091854
60.21712	87	0.4375	0.125	0.143868	0.121441
60.70985	88	0.4375	0.1875	0.140637	0.180736
61.39748	89	0.4375	0.25	0.13901	0.242411
62.34296	90	0.4375	0.3125	0.139323	0.309929
65.45824	91	0.4375	0.4375	0.148734	0.486182
68.03883	92	0.4375	0.5	0.161109	0.618389
60.57393	93	0.5	0.0625	0.159237	0.063535
60.78981	94	0.5	0.09375	0.1573	0.094619
61.05167	95	0.5	0.125	0.155795	0.125686
61.36549	96	0.5	0.15625	0.154754	0.157105
61.73929	97	0.5	0.1875	0.154224	0.189303
62.70576	98	0.5	0.25	0.154949	0.258098
64.06801	99	0.5	0.3125	0.158809	0.33763
68.84838	100	0.5	0.4375	0.183576	0.573957
61.32352	101	0.5625	0.0625	0.169734	0.066064
62.00614	102	0.5625	0.125	0.168181	0.13225
62.4549	103	0.5625	0.15625	0.16837	0.166597
62.9926	104	0.5625	0.1875	0.169335	0.202606
69.64394	105	0.5625	0.375	0.206022	0.525232
62.18804	106	0.625	0.0625	0.1809	0.069859
62.63979	107	0.625	0.09375	0.181205	0.105429
63.18949	108	0.625	0.125	0.182427	0.142324
70.42252	109	0.625	0.3125	0.228539	0.470884
63.27944	110	0.6875	0.0625	0.194186	0.075612
63.96806	111	0.6875	0.09375	0.196905	0.115545
75.99445	112	0.78125	0.1875	0.331237	0.412111
76.70606	113	0.8125	0.15625	0.350428	0.367799
77.47064	114	0.84375	0.125	0.371359	0.317084
78.30318	115	0.875	0.09375	0.394544	0.258123
79.22268	116	0.90625	0.0625	0.420668	0.188343
80.25911	117	0.9375	0.03125	0.450774	0.104096

It should be pointed out that this 2-D superset is different from the 4-D superset identified earlier. In fact, the 4-D superset is a subset of the 2-D superset (when the latter is considered in the 4-D space).

To approximate solution of the ILP for $AR_{\{\alpha_i^Y\}_{i=1}^{Q},\{(\alpha_i^U,x_i^U)\}_{i=1}^{S}}$ quantification, we consider only a finite number of values for the network outlet mole fractions and the VLE separator sub-vector parameters. Again, for the ith VLE separator, outlet 1 species 1 and species 2 mole fractions $\left(x^W_{i,1,1},x^W_{i,1,2}\right)$ are chosen as the two design parameters. Discretization levels of 1/16, 1/32, 1/64, and 1/128 for $\left(x^W_{i,1,1},x^W_{i,1,2}\right)$ and for the network outlets $\left(x^Y_{1,1},x^Y_{1,2}\right)$ are employed.

The 2-D approximate ARs for the above discretization levels are all illustrated graphically in Figure 3. Additionally, the AR superset is also depicted. Table 6 shows the vertex points for the approximate AR corresponding to the 1/128 discretization level.

The boundary of the true AR is guaranteed to be within the region contained by the boundary of the aforementioned

Table 9. Results of Parametric Studies of a Simple Distillation Column in UniSim®

# Trays	Feed tray position	# Trays above feed	# Trays below feed	Reflux ratio	Distillate acetone comp.
25	3	2	22	0	0.596756604
25	3	2	22	1	0.69290963
25	3	2	22	2	0.719580207
25	3	2	22	3	0.733660614
25	3	2	22	4	0.742608904
25	6	5	19	0	0.596588873
25	6	5	19	1	0.719300816
25	6	5	19	2	0.750379827
25	6	5	19	3	0.763731175
25	6	5	19	4	0.771347702
25	13	12	12	0	0.596575181
25	13	12	12	1	0.732117303
25	13	12	12	2	0.765637396
25	13	12	12	3	0.778979495
25	13	12	12	4	0.784957494
25	19	18	6	0	0.59665144
25	19	18	6	1	0.734567639
25	19	18	6	2	0.76830466
25	19	18	6	3	0.781019148
25	19	18	6	4	0.787605023
25	22	21	3	0	0.595805599
25	22	21	3	1	0.732134603
25	22	21	3	2	0.76472788
25	22	21	3	3	0.779578871
25	22	21	3	4	0.787220476
50	5	4	45	0	0.596587976
50	5	4	45	1	0.71357069
50	5	4	45	2	0.744024932
50	5	4	45	3	0.757675289
50	5	4	45	4	0.765238536
50	13	12	37	0	0.596578753
50	13	12	37	1	0.732224234
50	13	12	37	2	0.766144438
50	13	12	37	3	0.778791336
50	13	12	37	4	0.78524047
50	25	24	25	0	0.596572648
50	25	24	25	1	0.735949055
50	25	24	25	2	0.770035129
50	25	24	25	3	0.783567011
50	25	24	25	4	0.7899851
50	37	36	13	0	0.596511411
50	37	36	13	1	0.736942844
50	37	36	13	2	0.769646812
50	37	36	13	3	0.785146944
50	37	36	13	4	0.792047096
50	45	44	5	0	0.596520563
50	45	44	5	1	0.736292821
50	45	44	5	2	0.769239193
50	45	44	5	3	0.784236835
50	45	44	5	4	0.794275394
100	10	9	90	0	0.596587587
100	10	9	90	1	0.729024921
100	10	9	90	2	0.762710616
100	10	9	90	3	0.77545517
100	10	9	90	4	0.782004306
100	25	24	75	0	0.596587445
100	25	24	75	1	0.735834554
100	25	24	75	2	0.769608684
100	25	24	75	3	0.783744554
100	25	24	75	4	0.790271882
100	50	49	50	0	0.596586361
100	50	49	50	1	0.737130428
100	50	49	50	2	0.770222776
100	50	49	50	3	0.786431363
100	50	49	50	4	0.79203461
100	75	74	25	0	0.596608569
100	75	74	25	1	0.737466898
100	75	74	25	2	0.7707908
100	75	74	25	3	0.785904529
100	75	74	25	4	0.783141159

TABLE 9. *Continued*

# Trays	Feed tray position	# Trays above feed	# Trays below feed	Reflux ratio	Distillate acetone comp.
100	90	89	10	0	0.59657444
100	90	89	10	1	0.737537181
100	90	89	10	2	0.772077564
100	90	89	10	3	0.787752129
100	90	89	10	4	0.794833514
200	20	19	180	0	–
200	20	19	180	1	0.735567183
200	20	19	180	2	0.770158511
200	20	19	180	3	0.78294468
200	20	19	180	4	0.787401031
200	50	49	150	0	–
200	50	49	150	1	0.737355276
200	50	49	150	2	0.771974554
200	50	49	150	3	0.786931513
200	50	49	150	4	0.793442207
200	100	99	100	0	–
200	100	99	100	1	0.737574308
200	100	99	100	2	0.772119198
200	100	99	100	3	0.78716742
200	100	99	100	4	0.795083657
200	150	149	50	0	–
200	150	149	50	1	0.737613256
200	150	149	50	2	0.772146847
200	150	149	50	3	0.787199193
200	150	149	50	4	0.795113556
200	180	179	20	0	–
200	180	179	20	1	0.737625071
200	180	179	20	2	0.772160846
200	180	179	20	3	0.787865945
200	180	179	20	4	0.795099506

material balance derived superset, and the largest AR approximant provided by IDEAS.

Discussion/Conclusions

In the 4-D case study presented above, both numerical and graphical representations are shown, of a one-inlet, three-outlet VLE separator network AR. The numerical and graphical AR representations in Table 5 and Figure 2 can be utilized to rigorously address a variety of questions that a design engineer may pose.

"Is a particular combination of product compositions attainable by some one-inlet, three-outlet VLE separator network with the given flow rate specifications?" For example, consider the following product compositions: $\left[x^Y_{1,1}\ x^Y_{1,2}\ x^Y_{1,3}\right]^T=\left[0.2969\ 0.3125\ 0.3906\right]^T$, $\left[x^Y_{2,1}\ x^Y_{2,2}\ x^Y_{2,3}\right]^T=\left[0.156275\ 0.46875\ 0.374975\right]^T$, $\left[x^Y_{3,1}\ x^Y_{3,2}\ x^Y_{3,3}\right]^T=\left[0.446825\ 0.26875\ 0.284425\right]^T$. To answer whether a one-inlet, three-outlet VLE separator network with outlet product flow rates equal to 1 mol/s and these product compositions exists, one can identify using linear programming whether the point $(0.2969, 0.3125, 0.156275, 0.46875)$ under consideration can be written as a convex combination of the vertices identified in Table 5. For this example, this is indeed the case, as the above point can be written as an equally weighted combination of vertices 1, 8, 61, and 62. Graphically, as illustrated in Figure 4, the point under consideration is the midpoint of the segment defined by the midpoints of the segments connecting vertices 61 and 8, and vertices 62 and 1, respectively, in each of the two ternary diagrams.

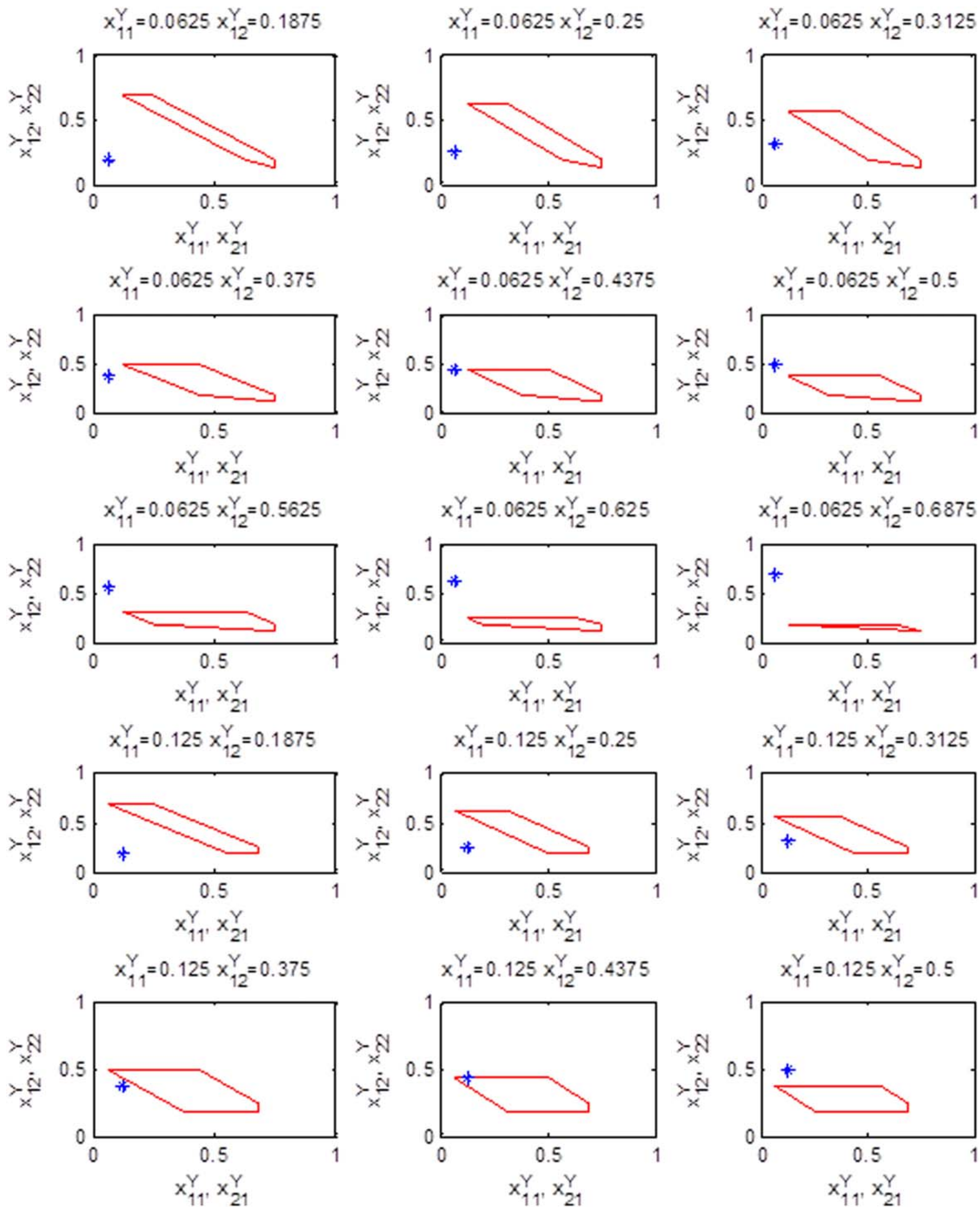

Figure A1. 2-D projections of the 4-D approximate AR, set 1.

[Color figure can be viewed in the online issue, which is available at wileyonlinelibrary.com.]

"What is the highest mole fraction of acetone that is attainable by some one-inlet, three-outlet VLE separator network with the given flow rate specifications?" Consulting Table 5 and Figure 2, suggests that product streams with flow rates all equal to 1 mol/s and compositions $\left[x_{1,1}^Y\ x_{1,2}^Y\ x_{1,3}^Y\right]^T=[0.0313\ 0.125\ 0.8437]^T$, $\left[x_{2,1}^Y\ x_{2,2}^Y\ x_{2,3}^Y\right]^T=[0.0313\quad 0.875\ 0.0937]^T$, $\left[x_{3,1}^Y\ x_{3,2}^Y\ x_{3,3}^Y\right]^T=[0.8374\ 0.05\ 0.1126]^T$ are attainable. In turn, this suggests that there exists a network that can deliver a product stream with flow rate 1 mol/s and an acetone mole fraction of 0.8437. This acetone mole fraction is higher than the acetone mole fraction (0.791) of the acetone/methanol binary azeotrope. The IDEAS methodology is in fact able to identify such a feasible separator network; it is presented in Tables 7 and 8, in Appendix B. Table 7 shows all network streams, including their inlet/outlet/VLE separator destinations and sources, and each stream's flow rate. Table 8 lists all VLE separators employed in the network, with their operating temperatures and exit compositions. The network generated incorporates several columns of various sizes, and other complex structures.

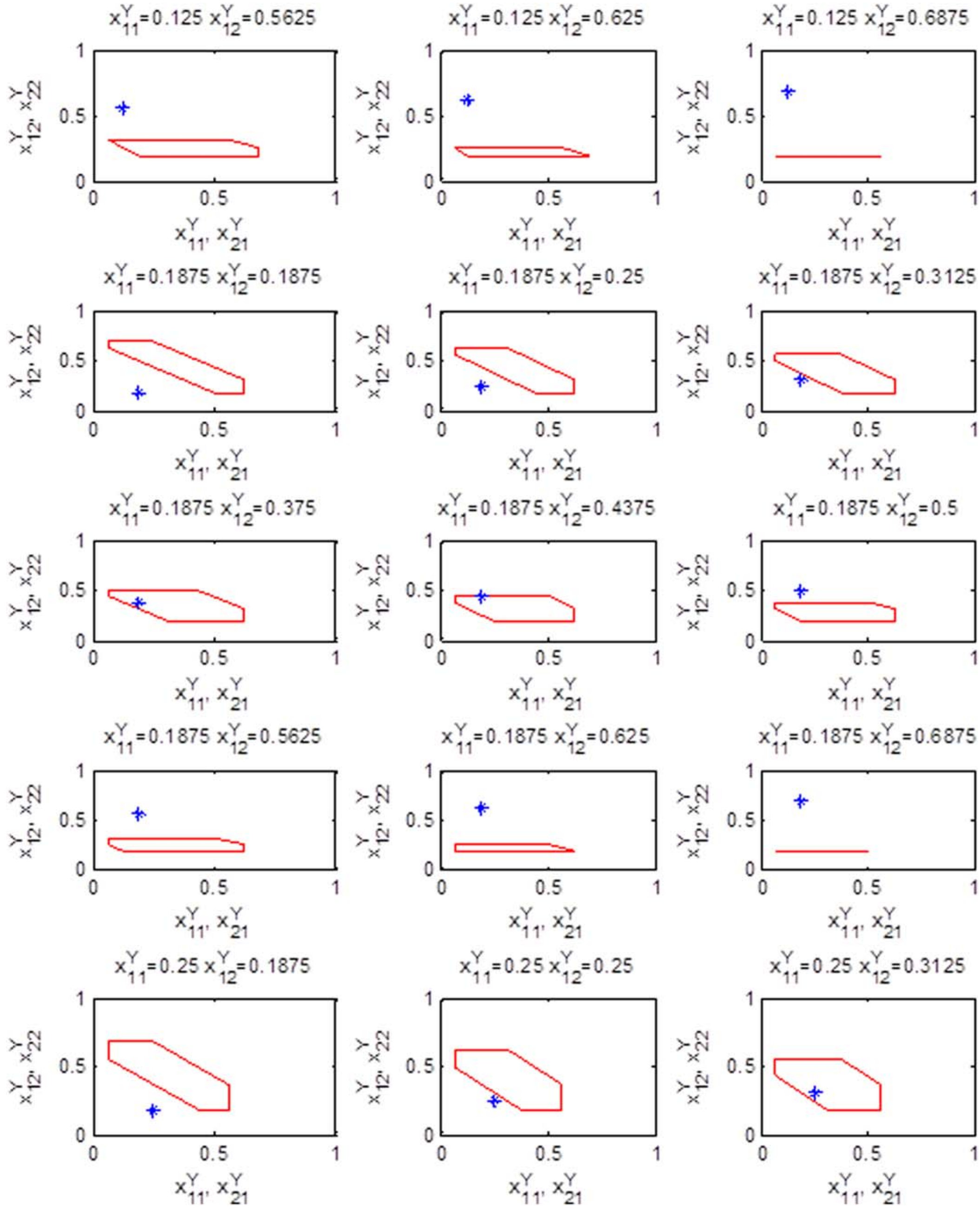

Figure A2. 2-D projections of the 4-D approximate AR, set 2.

[Color figure can be viewed in the online issue, which is available at wileyonlinelibrary.com.]

In the 2-D case study presented above, Figure 3 shows graphical representations of one-inlet, two-outlet VLE separator network AR approximants for discretization levels of 1/16, 1/32, 1/64, and 1/128. In addition, the AR superset is also depicted. This graphical representation can be utilized to rigorously address a variety of questions that a design engineer may pose.

"Is a particular combination of product compositions attainable by some one-inlet, two-outlet VLE separator network with the given flow rate specifications?" In this case, the answer can be obtained through simple inspection as to whether the composition under consideration belongs to the AR identified in Figure 3.

"What is the highest mole fraction of acetone that is attainable by some one-inlet, two-outlet VLE separator network with the given flow rate specifications?" Consulting Table 6 and Figure 3, suggests that product streams with flow rates equal to 1 mol/s and 2 mol/s and compositions $\left[x^Y_{1,1}\ x^Y_{1,2}\ x^Y_{1,3}\right]^T=\left[0.0625\ 0.03125\ 0.90625\right]^T$ and $\left[x^Y_{2,1}\ x^Y_{2,2}\ x^Y_{2,3}\right]^T=\left[0.41875\ 0.509375\ 0.071875\right]^T$, respectively, are attainable. In turn, this suggests that there exists a network that can deliver a product stream with flow rate equal to 1 mol/s and an acetone mole fraction of 0.90625. This acetone mole fraction is higher than the acetone mole fraction (0.791) of the acetone/methanol binary azeotrope, and is higher than the highest acetone mole fraction 0.8437 of the 4-D AR. As a simple distillation column is a one-inlet two-outlet VLE separation network, the 2-D AR should contain all compositions attainable by a simple distillation column

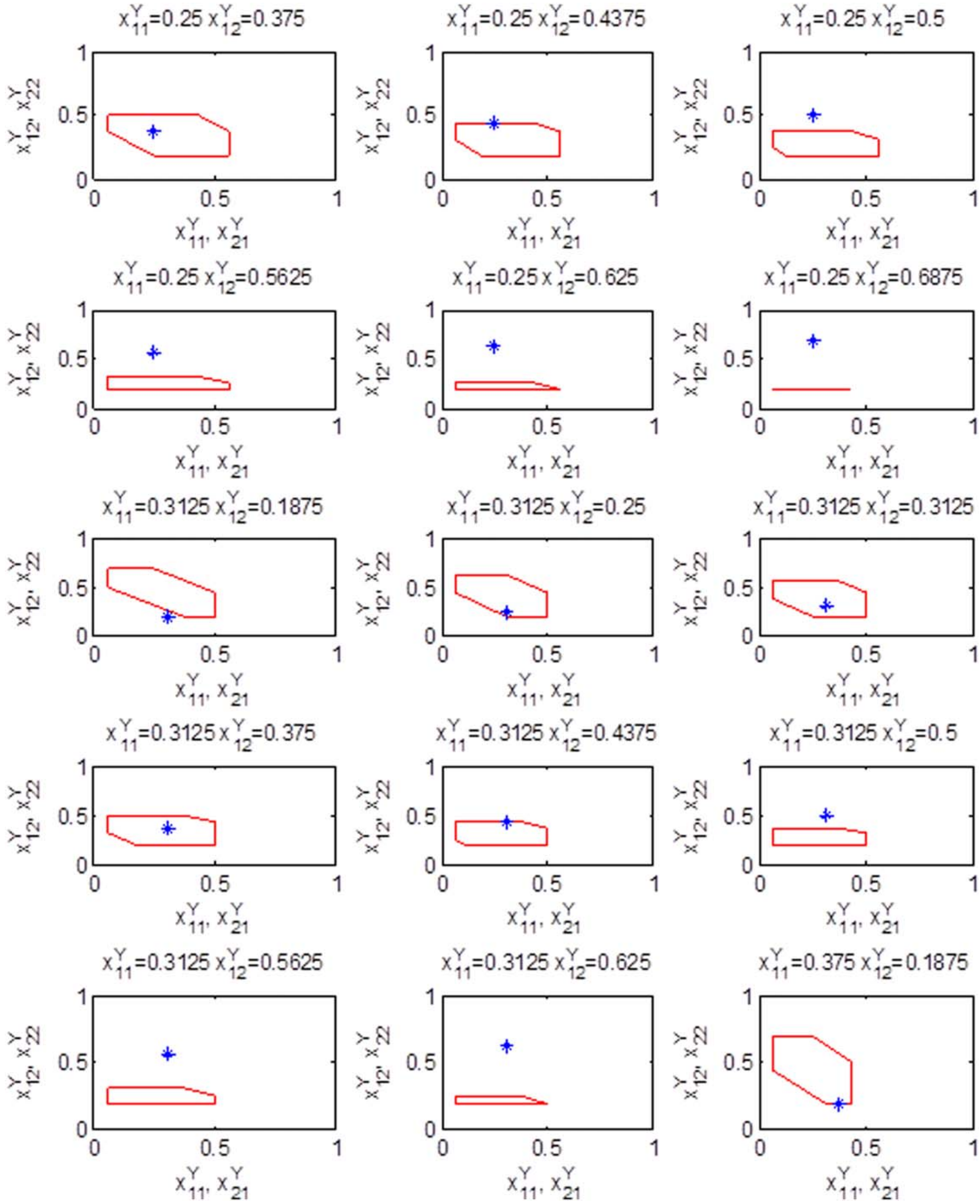

Figure A3. 2-D projections of the 4-D approximate AR, set 3.

[Color figure can be viewed in the online issue, which is available at wileyonlinelibrary.com.]

with specified top and bottom flow rate production. Indeed, an extensive parametric study was carried out in commercial simulator UniSim® by Honeywell. The results of the study are summarized in Table 9 in Appendix C, and suggest that the highest acetone mole fraction that can be attained by a conventional distillation column is 0.795. This confirms that the 2-D AR encompasses all product compositions attainable by a simple distillation column.

Appendix A illustrates how the 2-D projections of the 4-D AR evolve as the stream 1 compositions change. For example, the first nine templates of Appendix A illustrate these 2-D projections for the second stream outlet compositions as $x^Y_{1,2}$ varies from 0.1875 to 0.6875 for $x^Y_{1,1}=0.0625$. As expected from physical intuition, at the endpoints of the $x^Y_{1,2}$ interval, the region of possible stream 2 mole fractions is smaller than those for the interval's interior points. In addition, as the value of $x^Y_{1,2}$ increases, the range of $x^Y_{2,2}$ in the 2-D projection decreases, where at $x^Y_{1,2}=0.6875$, $x^Y_{2,2}$ is effectively fixed.

The proposed process network AR framework with inlet/outlet flow rate ratio specifications is a novel concept that allows the quantification of all attainable compositions by general process networks that feature multiple inlets and outlets and possess known feed and product flow rate ratios. The aforementioned AR is shown rigorously to be a convex set in an appropriately defined composition space. In turn, this convexity property is crucial in identifying increasingly accurate approximants of the process network AR through application of the IDEAS conceptual framework.

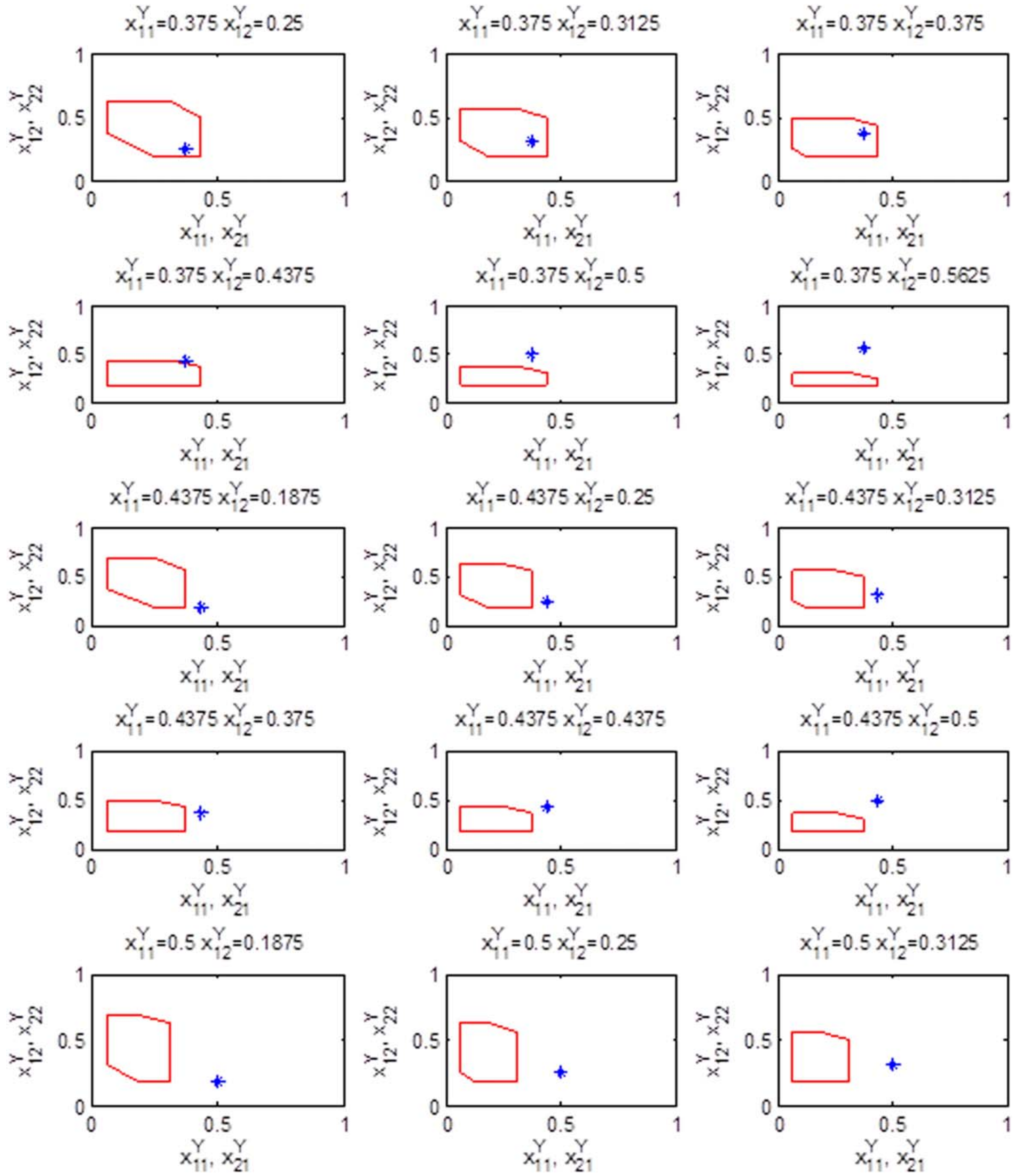

Figure A4. 2-D projections of the 4-D approximate AR, set 4.

[Color figure can be viewed in the online issue, which is available at wileyonlinelibrary.com.]

Having elaborated on the novel concept of process network AR, it is important to also comment on the IDEAS conceptual framework, which plays such a key role in the quantification of the aforementioned AR. The IDEAS framework is applicable to the general process network synthesis problem. To date, we have not yet identified a single chemical process to which the framework is not applicable. The computational complexity of IDEAS grows with the number of variables needed to specify the performance of a process unit. This number is typically equal to the number of species and process unit design variables. Therefore, the approach can be effectively employed for the design of complex systems, as long as the number of species present in these systems is not large.

The IDEAS model can be written as an equation $Ax = b$ involving the linear transformation A from one infinite-dimensional space to another. The domain of A is the nonnegative orthant of the space of absolutely summable sequences whose elements are the network flows. It is also true that the resulting feasible region defined by $Ax{=}b, x \geq 0$ in this infinite-dimensional space is a convex set. However, the convexity of this aforementioned feasible region has nothing to do with the convexity of the AR defined here, which lives in the low-dimensional space whose dimension is $(N_s{-}1){\times}(N_c{-}1)$, where $\left(\frac{\text{mol}}{s}\right)$ is the number of network outlet streams, and N_c is the number of components (species). As various outlet concentrations are considered, the entries of b are altered, and feasibility of $Ax{=}b, x \geq 0$ is

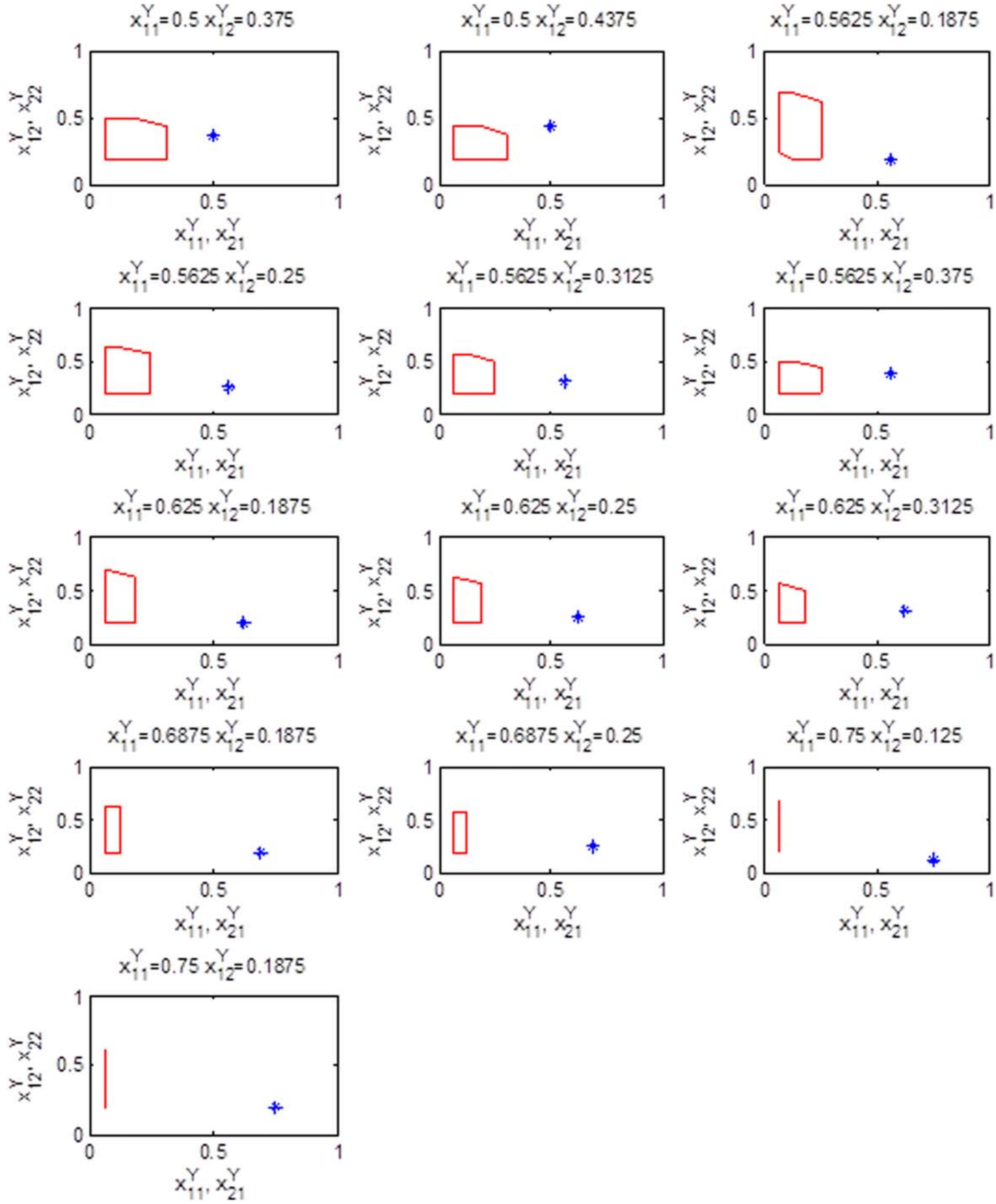

Figure A5. 2-D projections of the 4-D approximate AR, set 5.

[Color figure can be viewed in the online issue, which is available at wileyonlinelibrary.com.]

assessed. It is the union of all outlet concentrations that lead to feasible $Ax=b, x \geq 0$ that forms the AR introduced in this work, and is shown to be a convex subset of $\Re^{(N_s-1)\times(N_c-1)}$.

In this work, the novel concept of process network AR with inlet/outlet flow rate specifications was introduced. This work is applicable to a wide variety of systems, including those with alternate components, multiple azeotropes, and reactive separation, and many other process units. An IDEAS-based problem formulation of AR construction for process networks with units possessing any number of inlets and outlets was provided, and it was shown how to adapt the formulation to AR construction for VLE separator based networks. We have proven analytically the convexity of the AR, allowing for compact representation of its shape via vertex identification. A case study was carried out, illustrating the calculation of the VLE separator network AR for a ternary mixture by solving repeatedly IDEAS feasibility problems for all network outlet mole fractions belonging to a predefined AR superset.

Acknowledgments

Financial support for this work through NSF Grant NSF-CBET 0829211 is gratefully acknowledged. The authors

also acknowledge Paul Ghougassian for programming consultations in relation to the IDEAS algorithm used in this work.

Notation

Symbols

α_i^U = molar flow rate ratio of the ith process network inlet stream, $i=1,S$

α_i^Y = molar flow rate ratio of the ith process network inlet stream, $i=1,Q$

Letters

$f_{i,j}^X$ = species molar flow rate vector $\left(\left[\frac{\text{mol }1}{\text{s}}\cdots\frac{\text{mol }n}{\text{s}}\right]^{\text{T}}\right)$ inlet to the jth inlet stream of the ith process unit in OP, $j=1,s \quad i=1,\infty$

F_j^U = total molar flow rate of the jth network inlet stream, $j=1,S$, mol/s

$F_{i,j}^W$ = total molar flow rate of the jth outlet stream from the ith process unit in OP, $j=1,q \quad i=1,\infty$, mol/s

$F_{i,j}^X$ = total molar flow rate of the jth inlet stream to the ith process unit in OP, $j=1,s \quad i=1,\infty$, mol/s

F_j^Y = total molar flow rate of the jth network outlet stream, $j=1,Q$, mol/s

$F_{j,i}^{YU}$ = total molar flow rate to the jth network outlet stream from the ith network inlet stream, $j=1,Q \quad i=1,S$, mol/s

$F_{j,i,k}^{YW}$ = total molar flow rate to the jth network outlet stream from the kth outlet stream of the ith process unit, $j=1,Q, \quad i=1,\infty \quad k=1,q$, mol/s

$F_{i,k,j}^{XU}$ = total molar flow rate to the kth inlet stream of the ith process unit from the jth network inlet stream, $i=1,\infty \quad k=1,s \quad j=1,S$, mol/s

$F_{j,l,i,k}^{XW}$ = total molar flow rate to the lth inlet stream of the jth process unit from the kth outlet stream of the ith process unit, $j=1,\infty \quad l=1,s \quad i=1,\infty \quad k=1,q$, mol/s

P = pressure, bar

q = total number of outlets to each process unit in the process network

Q = total number of outlet streams from the IDEAS process network

R = gas constant, $\left(8.314\,\frac{\text{L}\cdot\text{kPa}}{\text{mol}\cdot\text{K}}\right)$

s = total number of inlets to each process unit in the process network

S = total number of inlet streams to the IDEAS process network

T = temperature, (K)

x_j^U = molar fraction vector of the jth network inlet stream, $j=1,S$

$x_{i,j}^W$ = molar fraction vector of the jth liquid outlet stream from the ith process unit in OP, $j=1,q \quad i=1,\infty$

x_j^Y = molar fraction vector of the jth network outlet stream, $j=1,Q$

$x_{i,j}^X$ = molar fraction vector of the jth inlet stream to the ith process unit in OP, $j=1,s \quad i=1,\infty$

Superscripts

U = network inlet

X = process unit inlet

Y = network outlet

W = process unit outlet

Literature Cited

1. Horn F. Attainable and non-attainable regions in chemical reactor technique. In: Proceedings of the Third European Symposium on Chemical Reaction Engineering. London: Pergamon Press, 1964: 123–138.
2. Glasser D, Crowe C, Hildebrandt D. A geometric approach to steady flow reactors: the attainable region and optimization in concentration space. *Ind Eng Chem Res*. 1987;26(9):1803–1810.
3. Hildebrandt D, Glasser D, Crowe CM. Geometry of the attainable region generated by reaction and mixing: with and without constraints. *Ind Eng Chem Res*. 1990;29(1):49–58.
4. Manousiouthakis V, Justanieah AM, Taylor L. The Shrink–Wrap algorithm for the construction of the attainable region: an application of the IDEAS framework. *Comput Chem Eng*. 2004;28(9):1563–1575.
5. Zhou W, Manousiouthakis V. Non-ideal reactor network synthesis through IDEAS: attainable region construction. *Chem Eng Sci*. 2006; 61(21):6936–6945.
6. Zhou W, Manousiouthakis V. Variable density fluid reactor network synthesis—construction of the attainable region through the IDEAS approach. *Chem Eng J*. 2007;129(1–3):91–103.
7. Davis B, Taylor L, Manousiouthakis V. Identification of the attainable region for batch reactor networks. *Ind Eng Chem Res*. 2008; 47(10):3388–3400.
8. Abraham TK, Feinberg M. Kinetic bounds on attainability in the reactor synthesis problem. *Ind Eng Chem Res*. 2004;43(2):449–457.
9. Posada A, Manousiouthakis V. Multi-feed attainable region construction using the Shrink-Wrap algorithm. *Chem Eng Sci*. 2008;63(23): 5571–5592.
10. Burri JF, Wilson SD, Manousiouthakis VI. Infinite-dimensional state-space approach to reactor network synthesis: application to attainable region construction. *Comput Chem Eng*. 2002;26(6):849–862.
11. Zhou W, Manousiouthakis V. On dimensionality of attainable region construction for isothermal reactor networks. *Comput Chem Eng*. 2008;32(3):439–450.
12. Zhou W, Manousiouthakis V. Automating the AR construction for non-isothermal reactor networks. *Comput Chem Eng*. 2009;33(1): 176–180.
13. Agarwal V, Thotla S, Mahajani SM. Attainable region of reactive distillation-Part I: single reactant non-azeotropic systems. *Chem Eng Sci*. 2008;63(11):2946–2965.
14. Agarwal V, Thotla S, Kaur R, Mahajani SM. Attainable region of reactive distillation. *Part II: single reactant azeotropic systems. Chem Eng Sci*. 2008;63(11):2928–2945.
15. Amte V, Nistala S, Malik R, Mahajani S. Attainable regions of reactive distillation—part III. *Complex reaction scheme: van de Vusse reaction. Chem Eng Sci*. 2011;66(11):2285–2297.
16. Amte V, Gaikwad R, Malik R, Mahajani S. Attainable region of reactive distillation—part IV: inclusion of multistage units for complex reaction schemes. *Chem Eng Sci*. 2012;68(1):166–183.
17. Doherty M, Malone M. Conceptual Design of Distillation Systems, New York: McGraw Hill, 2001.
18. Jobson M, Hildebrandt D, Glasser D. Attainable products for the vapour-liquid separation of homogeneous ternary mixtures. *Chem Eng J*. 1995;59:51–70.
19. Nisoli A, Malone MF, Doherty MF. Attainable regions for reaction with separation. *AIChE J*. 1997;43(2):374–387.
20. Smith JM, Van Ness HC, Abbott MM. Introduction to Chemical Engineering Thermodynamics, 7th ed. New York: McGraw-Hill, 2005:545.

Appendix A

Figures A1–A5 show 2-D projections of the 4-D approximate AR quantified using 1/16 discretization for $\left(x_{1,1}^Y, x_{1,2}^Y, x_{2,1}^Y, x_{2,2}^Y\right)$, $\left(x_{i,1,1}^W, x_{i,1,2}^W\right)$.

Appendix B

Tables 6 and 7 list an IDEAS-generated feasible VLE network configuration for the point product streams with flow rates all equal to 1 mol/s and compositions $\left[x_{1,1}^Y\ x_{1,2}^Y\ x_{1,3}^Y\right]^T=[0.0313\ 0.125\ 0.8437]^T$, $\left[x_{2,1}^Y\ x_{2,2}^Y\ x_{2,3}^Y\right]^T=[0.0313\ 0.875\ 0.0937]^T$, $\left[x_{3,1}^Y\ x_{3,2}^Y\ x_{3,3}^Y\right]^T=[0.8374\ 0.05\ 0.1126]^T$. Table 6 shows all network streams, including their inlet/outlet/VLE separator destinations and sources, and each stream's flow rate. Table 7 lists all VLE separators employed in the network, with their operating temperatures and exit compositions.

Appendix C

An extensive parametric study was carried out in commercial simulator UniSim® by Honeywell to verify that the 2-D AR contains all compositions attainable by a simple distillation column with specified top and bottom flow rate production. The parameters for this study were the number of trays (25, 50, 100, 200), feed tray position (10%, 25%, 50%, 75%, and 90% of the number of trays), and reflux ratio (0, 1, 2, 3, 4). The results of the study are summarized in Table 9, and suggest that the highest acetone mole fraction that can be attained by a conventional distillation column is 0.795. This confirms that the 2-D AR encompasses all product compositions attainable by a simple distillation column.

Manuscript received Mar. 6, 2013, and revision received Sept. 3, 2013.